



National Library
of Canada

Acquisitions and
Bibliographic Services Branch

395 Wellington Street
Ottawa, Ontario
K1A 0N4

Bibliothèque nationale
du Canada

Direction des acquisitions et
des services bibliographiques

395, rue Wellington
Ottawa (Ontario)
K1A 0N4

Your file *Votre référence*

Our file *Notre référence*

NOTICE

The quality of this microform is heavily dependent upon the quality of the original thesis submitted for microfilming. Every effort has been made to ensure the highest quality of reproduction possible.

If pages are missing, contact the university which granted the degree.

Some pages may have indistinct print especially if the original pages were typed with a poor typewriter ribbon or if the university sent us an inferior photocopy.

Reproduction in full or in part of this microform is governed by the Canadian Copyright Act, R.S.C. 1970, c. C-30, and subsequent amendments.

AVIS

La qualité de cette microforme dépend grandement de la qualité de la thèse soumise au microfilmage. Nous avons tout fait pour assurer une qualité supérieure de reproduction.

S'il manque des pages, veuillez communiquer avec l'université qui a conféré le grade.

La qualité d'impression de certaines pages peut laisser à désirer, surtout si les pages originales ont été dactylographiées à l'aide d'un ruban usé ou si l'université nous a fait parvenir une photocopie de qualité inférieure.

La reproduction, même partielle, de cette microforme est soumise à la Loi canadienne sur le droit d'auteur, SRC 1970, c. C-30, et ses amendements subséquents.

Canada

UNIVERSITY OF ALBERTA

**The Three-Dimensional Vortex Structure of an Impacting
Water Drop**

BY



Bill James Peck

A thesis submitted to the Faculty of Graduate Studies and Research in partial fulfillment
of the requirements for the degree of Master of Science.

DEPARTMENT OF MECHANICAL ENGINEERING

EDMONTON, ALBERTA

SPRING 1993



National Library
of Canada

Acquisitions and
Bibliographic Services Branch

395 Wellington Street
Ottawa, Ontario
K1A 0N4

Bibliothèque nationale
du Canada

Direction des acquisitions et
des services bibliographiques

395, rue Wellington
Ottawa (Ontario)
K1A 0N4

Votre bibliothèque

Notre bibliothèque

The author has granted an irrevocable non-exclusive licence allowing the National Library of Canada to reproduce, loan, distribute or sell copies of his/her thesis by any means and in any form or format, making this thesis available to interested persons.

L'auteur a accordé une licence irrévocable et non exclusive permettant à la Bibliothèque nationale du Canada de reproduire, prêter, distribuer ou vendre des copies de sa thèse de quelque manière et sous quelque forme que ce soit pour mettre des exemplaires de cette thèse à la disposition des personnes intéressées.

The author retains ownership of the copyright in his/her thesis. Neither the thesis nor substantial extracts from it may be printed or otherwise reproduced without his/her permission.

L'auteur conserve la propriété du droit d'auteur qui protège sa thèse. Ni la thèse ni des extraits substantiels de celle-ci ne doivent être imprimés ou autrement reproduits sans son autorisation.

ISBN 0-315-82182-5

Canada

UNIVERSITY OF ALBERTA
RELEASE FORM

NAME OF AUTHOR: Bill James Peck

TITLE OF THESIS: The Three-Dimensional Vortex Structure of an Impacting Water Drop.

DEGREE: Master of Science

YEAR THIS DEGREE GRANTED: 1993

Permission is hereby granted to the University of Alberta Library to reproduce single copies of this thesis and to lend or sell such copies for private, scholarly or scientific research purposes only.

The author reserves all other publication and other rights in association with the copyright in the thesis, and as hereinbefore provided neither the thesis nor any substantial portion thereof may be printed or otherwise reproduced in any material form whatever without the author's prior written permission.

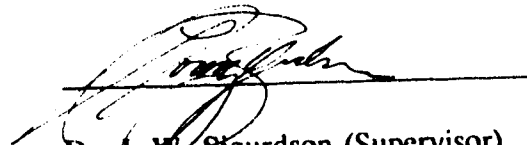


Box 1055
Sylvan Lake, Alberta,
Canada.
T0M-1Z0

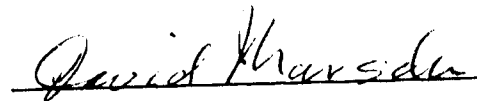
Date: _____

UNIVERSITY OF ALBERTA
FACULTY OF GRADUATE STUDIES AND RESEARCH

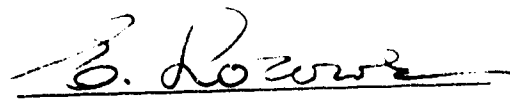
The undersigned certify that they have read, and recommend to the Faculty of Graduate Studies and Research for acceptance, a thesis entitled **The Three-Dimensional Vortex Structure of an Impacting Water Drop** submitted by Bill James Peck in partial fulfillment of the requirements for the degree of Master of Science.



Dr. L.W. Sigurdson (Supervisor)



Dr. D.J. Marsden



Dr. E.P. Lozowski

Date: JAN 28, 1993

Abstract

Observations are reported of the three-dimensional vortex structure created by a dyed water drop impacting upon a pool of water. The structure and evolution of the vorticity is studied for a very specific Weber and Froude number regime. The drop and pool do not make first contact at the bottom of the drop but at latitudes away from the bottom pole of the drop. This traps a thin, curved, pancake-shaped air bubble beneath the drop which rapidly contracts into a sphere. As the drop impacts the pool its impulse produces vorticity which rolls up into a vortex ring. As the vortex ring travels down through the pool, fluid is drawn from the central axis of the vortex ring to form a "stalk". This reaches from the primary ring to another ring of vorticity which has formed in the now reversing free surface impact crater. As the primary ring convects downward its diameter contracts and some vortex-filaments undergo an azimuthal instability which grows until they escape the trapped orbits of the primary vortex ring and are "shed". This results in three to five loops or "petals" left behind the primary ring. A three-dimensional vortex skeleton of this structure is presented. The results confirm the hypothesis that the structure is topologically similar to that of the separation bubble on a blunt flat plate. The structure's appearance is also strikingly similar to the appearance of an above-ground atomic blast. The production and interaction of vorticity at a free surface is also discussed.

Acknowledgements

The author acknowledges his supervisor, Dr. L.W. Sigurdson, for guidance and also for financial support through a grant provided by the Natural Sciences and Engineering Research Council, grant number OGP0041747. Financial support was also provided by the University of Alberta's SEED program, grant number 28300. Mr. B. Faulkner and Mr. I. Williamson are to be thanked for their assistance in construction of the apparatus and computer programming. Thanks also go to the staff of the Mechanical Engineering machine shop especially Mr. M. Schubert. It was only because of their immeasurable patience and high level of craftsmanship that this study was successful.

Table of Contents

Chapter 1. Introduction	1
References for Chapter 1	4
Chapter 2. The Experiment, Results and Discussion	5
2.1. Literature review	5
2.2. The Experiment	8
2.2.1. <i>Stage-1 apparatus</i>	9
2.2.2. <i>Stage-2 apparatus</i>	10
2.2.3. <i>Stage-3 apparatus</i>	10
2.2.4. <i>Cleaning procedures</i>	12
2.2.5. <i>Photography and timing</i>	12
2.3. Experimental Sensitivity	14
2.4. Experimental Results	16
2.4.1. <i>The falling drop</i>	17
2.4.2. <i>Drop impact and air bubble formation</i>	17
2.4.3. <i>Birth of the vortex structure</i>	19
2.4.4. <i>The onset of instability</i>	21
2.4.5. <i>Relaminarization and phase lock</i>	22
2.5. Discussion	23
2.5.1. <i>Vorticity generation</i>	23
2.5.2. <i>Vortex model</i>	26
2.5.3. <i>Similarity to other flow topologies</i>	28
References for Chapter 2	30
Chapter 3. Conclusions and Suggestions for Further Work	46
3.1. Conclusions	46
3.2. Suggestions for further work	47
References for Chapter 3	50

Appendices

Appendix 1. Automation of the Apparatus and Computer Program Listing . .	51
Appendix 2. Determination of the Vortex Ring Reynolds Number	85
Appendix 3. Vortex Dynamics and Vorticity Generation at a Free Surface . .	89
<i>A3.1 Vortex dynamics overview</i>	<i>89</i>
<i>A3.2 Vorticity generation at a free surface</i>	<i>94</i>

List of Tables

Table 1. Summary of experimental conditions	33
---	----

List of Figures

Figure 2.1. Apparatus	34
Figure 2.2. Viewing positions	35
Figure 2.3. Laser optic alignment	35
Figure 2.4. Aspect ratio vs. fall height	36
Figure 2.5. Profile of free surface vs. time	37
Figure 2.6.(a). Secondary structure	38
Figure 2.6.(b). Idealized secondary structure	38
Figure 2.7. Three-dimensional vortex skeleton	39
Figure 2.8. Two dimensional section of vortex skeleton	40
Figure 2.9. Trapped streamlines of the primary ring and base rings	41
Figure A2.1. Multiple exposure photograph of vortex ring	56
Figure A2.2. Vortex ring geometry	56
Figure A2.3. Velocity of vortex ring vs. time	57
Figure A3.1. Coordinate system at free surface	62
Figure A3.2. Region of curvature at a free surface	62
Figure A3.3. Sketch of flow geometry	63
Figure A3.4. Sketch of equivorticity lines	63

List of Plates

Plate 2.1. Top view of drop impact, $t < 1$ ms.,	42
Plate 2.2. Top view of drop impact, $t = 1$ ms.,	42
Plate 2.3. Axial view of drop created vortex structure, $t = 14$ ms.,	42
Plate 2.4. Axial view of drop created structure. $t = 19$ ms.,	42
Plate 2.5. Axial view of drop created structure, $k = 3$, $t = 65$ ms.,	42
Plate 2.6. Axial view of drop created structure, $k = 4$, $t = 65$ ms.,	42
Plate 2.7. Side view of impinging drop, $t < 1$ ms.,	43
Plate 2.8. Side view of impinging drop, $t = 2.5$ ms.,	43
Plate 2.9. Side view of drop created vortex structure, $t = 7.5$ ms.,	43
Plate 2.10. Side view of drop created vortex structure, $t = 9.0$ ms.,	43
Plate 2.11. Side view of drop created vortex structure, $t = 13$ ms.,	43
Plate 2.12. Side view of drop created vortex structure, $t = 16$ ms.,	43
Plate 2.13. Side view of drop created vortex structure, $t = 20$ ms.,	44
Plate 2.14. Side view of drop created vortex structure, $t = 30$ ms.,	44
Plate 2.15. Side view of drop created vortex structure, $t = 50$ ms.,	45
Plate 2.16. Side view of drop created vortex structure, $t = 65$ ms.,	45

Symbols and Nomenclature

Roman Symbols

D	Water drop diameter (based on a sphere)
D_H	Diameter of a horizontal section through the water drop
D_V	Vertical diameter
Fr	Froude number, $Fr = \frac{u^2}{gD}$
g	Acceleration due to gravity
I	Hydrodynamic impulse vector
k	Azimuthal wavenumber
K	Diffusivity
n	Normal axis at free surface
q	Magnitude of tangential fluid velocity
r	Radial axes from vortex ring's axis of symmetry
\mathbf{r}	Position vector
R	Radius to the azimuthal axis of vortex ring core
Re	Vortex ring Reynolds number, $Re = \frac{\Gamma}{\nu}$
s	Tangential axis at free surface
Sc	Schmidt number, $Sc = \frac{\nu}{K}$
t_c	Cancellation time scale
u	Impact velocity of water drop
u_T	Terminal velocity of a falling water drop
U_{ring}	Vortex ring velocity
V	Volume of water drop
We	Weber number, $We = \frac{\rho u^2 D}{\gamma}$
x	Axis coincident with vortex ring axis of symmetry
x_s	Axis tangent to free surface

y_*	Axis normal to free surface
z	Fall height of water drop

Greek Symbols

Γ	Circulation
γ	Surface tension
δ	Vortex core radius
ϵ	Strain rate
θ	Angle of incidence between axes at free surface
κ	Surface curvature
ν	Kinematic viscosity
μ	Dynamic viscosity
ρ	Fluid density
τ	Period of oscillation
τ_{ns}	Off-diagonal shear stress
ϕ	Azimuthal angle
Ω	Angular velocity
ω	Vorticity

Chapter 1. Introduction

Recently, large scale coherent structures have been identified within the apparent chaos of some turbulent flows. These structures are essentially regions of concentrated vorticity within the flow. Among the first researchers to discover the existence of these structures were Brown and Roshko (1973). In their work, the now-famous structure within the turbulent mixing layer was identified. By modelling the mixing layer as a series of span-wise aligned vortices the previously well-known mean velocity field and mixing layer growth rate characteristics were satisfied with remarkable simplicity. Saffman states that it is now proposed that turbulence can be modelled as the creation, evolution, interaction and decay of vortical structures. He summarizes as follows, "It can be claimed that the problems of turbulence and transition are problems of the mechanics of vorticity, which is the fundamental dynamical quantity and constitutes the 'sinews and muscles of fluid motion'" (Saffman 1980).

The identification of coherent structure within turbulence has fostered the idea of tracking the vorticity with time and constructing a model based on the topology of the constituent lines of vorticity^{*} (Sigurdson 1986). Using this approach many incompressible flows can then be thought of as the superposition of a distribution of line

* The terms vortex-line, vortex-filament, vortex-tube and line vortex are defined as follows. A vortex-line is a line which is everywhere tangent to the local vorticity; a vortex-tube is the surface formed by all the vortex-lines which pass through a closed curve drawn in the fluid; a vortex-filament is a vortex-tube of small but finite cross section; a line vortex is the contraction of a vortex-tube onto a single line while keeping its circulation constant. It should be noted here that a vortex-tube cannot end in the interior of a fluid. These are the definitions as defined by Batchelor (1967). A vortex skeleton can then be thought of as an idealized characteristic structure constructed from line vortices.

vortices on a base potential flow. It is hoped that a simplified description of many flows can be achieved by identifying the characteristic vortex structure within them.

The present study was inspired by the remarkable similarity between the appearance of an atomic bomb mushroom cloud and the three-dimensional vortex structure created when a water drop impacts the free surface of a pool of water. The apparent similarity, despite a 6 order difference in Reynolds number, has previously been discussed by Sigurdson (1987, 1991). This comparison is an indication of how little the Reynolds number affects the qualitative large scale structure of a turbulent free shear flow. It also raises questions of why there is a similarity between the structures at all. To aid in answering these questions experiments have been undertaken to understand the birth and evolution of the vortex structure created by the impacting drop. An improved understanding of this has allowed the clarification and improvement of a previously proposed vortex skeleton structure (Peck and Sigurdson 1992, Sigurdson and Peck 1991). The present work contains a complete description of this revised structure. It is described by constructing a vortex skeleton consisting of five closed line vortices.

Impacting drops are also of interest for fundamental reasons. The drop-created structure may be one of the simplest three-dimensional vortex structures that can be isolated and studied in a controlled manner. It is also of interest as a contribution to the understanding of vorticity generation at a free surface.

Chapter 2 is presented in paper format. This chapter contains a literature review, a description of the experimental apparatus, observations and results. Plates 2.4, 2.6, 2.12 and 2.16 have appeared in the Physics of Fluids A "Gallery of Fluid Motion" (Peck and Sigurdson 1992). Plates 2.9, 2.12 and 2.15 have appeared in Discover and New Scientist magazines and are to appear in Current Science magazine. Plate 2.16 will appear on the cover of the journal Outlook on Agriculture.

Chapter 3 contains conclusions and recommendations for future work. Three appendices appear: Appendix 1 discusses the automation of the experiment in detail, Appendix 2 discusses the manner in which the vortex ring's Reynolds number was obtained and Appendix 3 gives an overview of vorticity dynamics and discusses the derivation of a kinematic vorticity constraint at a free surface.

References for Chapter 1

Batchelor G.K. 1967 *An Introduction to Fluid Dynamics*. Cambridge University Press.

Brown G.L. and Roshko A. 1973 On density effects and large structure in turbulent mixing layers. *J. Fluid Mech.* **64**, 775-816.

Current Science (to appear fall 1992).

Discover May 1992 **13**, 11.

New Scientist July 18, 1992 **18**, 18.

Outlook on Agriculture Fall 1992 **21**, covering page.

Peck B.J. and Sigurdson L.W. 1992 Gallery of Fluid Motion: Impacting water drops. *Phys. Fluids A* **4**, Helen Reed (ed.), 1872.

Saffman P.G. 1980 Vortex interactions and coherent structures in turbulence. *Proc. Symp. on Transition and Turbulence*. Academic Press, 149-166.

Sigurdson L.W. The structure and control of a turbulent reattaching flow. Ph.D. Thesis, Graduate Aeronautical Laboratories, California Institute of Technology, June, 1986.

Sigurdson L.W. 1987 The three-dimensional vortex structure of the starting vortex ring. *Bull. Am. Phys. Soc.* **32**, 2095.

Sigurdson L.W. 1991 Gallery of fluid motion: Atom bomb/water drop. *Phys. Fluids A* **3**, Helen Reed (ed.), 2034.

Sigurdson L.W. and Peck B.J. 1991 The structure created by an impacting water drop. *Bull Am. Phys. Soc.* **36**, 2619.

Chapter 2. The Experiment, Results and Discussion*

2.1. Literature review

Vortex rings produced by water drops impacting a free surface have been the topic of a variety of published studies for more than a century (Rogers 1858, Thomson and Newall 1885). The deceptive simplicity of this classic experiment allows it to be observed with the most casual apparatus, such as an eye-dropper releasing a dyed water drop into a pool. If released from not too great a height an exquisite vortex ring is formed from the dyed drop's fluid which then travels down through the pool. It quickly becomes apparent that variations in the vortex ring's characteristics occur with slight changes in the drop's initial conditions.

Rogers (1858) discusses vortex rings formed by a variety of means including those produced by impacting drops. Later, Thomson and Newall (1885) produced an extensive paper centring wholly on the subject of drop-produced vortex rings using a variety of liquids. Both of these early studies were hindered by the lack of photographic apparatus to record such a small and rapid event. The first detailed photographs of an impacting water drop's structure were presented in Okabe and Inoue's work (1961). Two of these photographs appear in Batchelor (1967), one of which (Batchelor 1967 (Plate 7.2.3.1)) is the inspiration for the work presented here. This photograph exhibits a particularly beautiful three-dimensional structure reminiscent of an inverted flower. The photographs taken by Okabe and Inoue did not provide sufficient information to fully understand the three-dimensional topology of the structure created by the impacting drop. No published photographs containing this information were available in the literature.

*A version of this chapter has been submitted for publication. Peck and Sigurdson 1992. *Journal of Fluid Mechanics*.

This required the construction of the present experiment to obtain photographs of sufficient detail.

Although other research has been undertaken to gain insight into a variety of phenomena associated with drop-formed vortex rings, very little has been published which recognizes the complex topology that exists at early times.

Chapman and Critchlow (1967) undertook experiments to understand the effect of fall height on the penetration depth of drop-formed vortex rings using a variety of liquids. No reference was made to any resulting structure and no photographs were published of their experimental results. It was determined that the oscillation phase of the drop at impact plays a determining factor in the penetration depth of the vortex ring. The oscillations in the drop arise during its separation from the forming tip.

Keedy (1967) undertook experiments of a similar nature using a variety of liquids. The results were recorded using high speed cinematography and large format photographs which are included in his work. He too established the dependence of penetration depth on drop oscillation phase. He did not discuss the structure of the phenomenon in detail.

Rodriguez and Mesler (1988) also investigated the penetration depth of vortex rings as part of an ongoing effort to gain insight into secondary nucleation and boiling. The results published contradict the two earlier works just mentioned (Keedy 1967, Chapman and Critchlow 1967) with respect to which phase at drop impact produced the most penetrating vortex ring. Several quality photographs are published and a reference is given to the observation of "The plumes above the vortex ring ..." left in the wake of the ring at early times. These photographs did not reveal adequate detail of the structure in question.

Much effort has been expended trying to understand the production and interaction of vorticity with a free surface in other configurations. A great deal of work has dealt

with computational solutions of vortex pairs and rings rising towards a free surface. Willmarth et al. (1989) examine the problem of a counter-rotating two-dimensional pair approaching a free surface and compare the computed trajectories of the cores to experiments. Ryskin and Leal (1984 a, b, c) numerically investigate the problem of rising bubbles. Ohring and Lugt (1990) have investigated the case of a viscous two-dimensional vortex pair rising toward a free surface by computationally solving the Navier-Stokes equations. Both (Ryskin and Leal 1984 a, b, c, Ohring and Lugt 1990) discuss the role of the free surface curvature in the production of vorticity at the interface. Vortex rings rising towards a free surface have been studied experimentally by Bernal and Kwon (1989) The effect of surfactants in vortex-free-surface interaction was also considered. Trygvasson et al. (1992) provide a comprehensive review of ongoing research into surfactant effects on vortex-free-surface interactions.

The vortex ring in an unbounded fluid has been the topic of a great deal of research. Classical solutions are well known which describe the motion of ideal vortex rings (see for instance Lamb 1945) and more recently the effects of viscosity have been considered (Saffman 1970). Widnall and Sullivan (1973) and later Widnall, Bliss and Tsai (1974) have shown the vortex ring to be unstable and prone to develop azimuthal bending waves along the core. Maxworthy (1972, 1974) has published experimental results for laminar and turbulent vortex rings produced by ejecting fluid through an immersed orifice and suggested a model for the entrainment and expulsion of fluid by the ring. More recently Glezer and Coles (1990) have investigated the turbulent vortex ring and identified a particular structure within it. A comprehensive review of vortex rings with comments on drop-formed rings is now available (Shariff and Leonard 1992).

In the present work the experimental apparatus is described in §2.2. A short discussion of the sensitivity of the experiments follows in §2.3. In §2.4 the experimental

results and observations are presented. In §2.5 a proposed model for the three-dimensional vortex structure is discussed as well as free surface vorticity generation and the similarity of this flow with others.

2.2. The Experiment

Preliminary experiments were conducted using the apparatus described by Okabe and Inoue (1961) in an attempt to reproduce their results. This consisted of using 4.5 mm diameter drops (based on an "equivalent spherical diameter"), dyed with fluorescein, falling from the tip of a 25 mL burette situated 10 mm above the free surface. The primary source of data used to study the vortex structure created by the impacting drops was 35 mm photography. The evolution of the structure was determined from the examination of a composite sequence of these photographs taken at known times after impact. It was therefore essential that the vortex structure be reproducible for each drop to ensure that its evolution was accurately represented. The structure created by the 4.5 mm drops was very difficult to reproduce as a consequence of the widely varying nature of the drop separation from the burette tip and the resulting large oscillations of the falling drop. This rendered significant data collection impossible.

Very little information was available in the literature concerning the construction of an appropriate apparatus. Most previous experiments have been conducted with very rudimentary apparatus. As a result, the apparatus used in the present experiments has evolved through three stages. Each successive stage was constructed in an attempt to obtain more reproducible results. The three stages will be described in §2.2.1, §2.2.2 and §2.2.3, the cleaning procedures in §2.2.4 and photographic timing in §2.2.5.

2.2.1. Stage-1 apparatus

To obtain a more reproducible geometry at impact, smaller diameter water drops ($2.6 \text{ mm} \pm .1 \text{ mm}$) were released from a greater height (34.5-38 mm), thus maintaining a similar Weber number.* This created a more spherical drop and allowed the oscillations to decay somewhat before impact. The drops were manually produced on the end of a .40 mm diameter hypodermic tube mounted in a carrier fabricated from nalgene. The carrier was mounted on a micrometer fed three-axis traverse to allow precise positioning of the hypodermic tube in relation to the free surface. Mounting the hypodermic tube in this manner also ensured that the tubes longitudinal axis would remain vertical. Fluid was introduced into the hypodermic through a length of tygon tubing which was attached to a syringe that served as a manually operated pump. Drops were formed at a slow rate. The sizes of the drops produced were calculated by producing several and taking their average volume. The diameter was then calculated assuming the drops were spherical.

The test cell used to hold the pool of receiving water was constructed from flat pieces of glass cemented along the edges with a silicon adhesive to form a rectangular vessel. The test cell, a laser used for timing, the three axis traverse and the photographic equipment were mounted on optical benches to ensure proper alignment. The entire experiment was mounted on a small vibration-isolation optical-breadboard to stabilize the motion of the free surface. The photographic techniques used to collect the data and the timing methods are similar for all three stages and will be discussed in §2.2.4.

*The Weber number is defined in §2.3. In calculating the Weber number for the 4.5 mm drops the maximum velocity of the leading edge of the drop (with respect to its centroid) as it was passing from spherical to prolate was added to the velocity of the drop's centroid. This added a velocity of the same order as the impact velocity. For the 2.6 mm drops falling a greater distance this added velocity was $O(3\%)$ of the impact velocity and was neglected.

2.2.2. Stage-2 apparatus

The stage-1 apparatus was modified to obtain a more reproducible method of drop formation and to reduce wave motion on the free surface of the test cell fluid. To achieve the latter requirement it was found necessary to automate the experiment to eliminate the inevitable disturbances caused by human presence. As a result there was no need for human operation of any equipment once the experiment had begun. The entire experiment was now mounted on a large optical vibration-isolation table to isolate the experiment from floor vibration.

A personal computer was used to manage the experiment through a variety of I/O devices which would: automatically control a small pump used to form and release drops, operate the camera and strobe equipment, record cell and ambient temperatures and time delays between drop releases (Figure 2.1). The time between each drop release was at least 2 minutes to ensure that any disturbances present in the cell had time to dissipate.

To obtain a reproducible method of drop formation a small pump was fabricated. The pump consisted of a 3.2 mm diameter brass piston riding in a plexiglass bore. The piston was driven by a gear-reduced stepper motor which ensured precise control of the fluid delivery rate. Each drop's volume was calculated using the number of steps of the motor required to produce that drop. To form a 11.5 μL drop 1800 were required. The test cell used to hold the receiving pool was the same as the stage-1 unit as were the hypodermic tube carriers.

2.2.3. Stage-3 apparatus

The third iteration was initiated to allow the experiment to be cleaned using a rigorous cleaning procedure which will be outlined §2.2.4. This required modification of the pump and test cell.

A new pump was constructed to the same dimensions as the stage-2 pump using stainless steel and teflon. The same drive system was used to actuate the piston. The tubing used to deliver the dyed fluid to the hypodermic tubes was changed to a thick walled teflon tube to allow cleaning and to ensure the tube did not expand with the pressure produced by the pump.

The dyed drops were still formed on the end of a .40 mm diameter hypodermic tube. A technique was devised to prepare the tube which enhanced the reproducibility of the drop volume. The outer wall of the tube was highly polished. The end of the tube was ground flat, at right angles to the tube's length and was not polished. This technique allowed consistently sized drops to be produced, which did not creep up the sides of the hypodermic tube during formation. Having the pendant drop form in this way ensured that it released from the tube tip axisymmetrically resulting in a vertical trajectory during the fall. Drops which crept up the side of the tube on poorly prepared tips often acquired trajectories off vertical. The prepared tube was now mounted in a teflon carrier to facilitate cleaning. The teflon carrier was mounted on the same three-axis traverse used in the earlier stages.

A new 8.2 cm × 8.2 cm × 12.5 cm test cell was constructed of a single piece of blown glass. A circular, optically clear, 4.25 cm diameter window was fused into one wall of the vessel to enable proper focusing of the photographic equipment.

The results obtained with the stage-3 apparatus verified that the result from the stage-1 and 2 apparatus were valid as they were not qualitatively different. The stage 3 apparatus will be used for further experiments. A description of the computer program which runs the experiment is included in Appendix 1.

2.2.4. Cleaning procedures

The sensitivity of free surface experiments to surface contamination required strict cleaning procedures to be followed. All the components of the stage-3 apparatus which would come in contact with either the fluid in the test cell or the dyed fluid were constructed of teflon, stainless steel or glass which allowed the apparatus to be cleaned using the following technique adapted from the technique used by Smedley and Coles (1989). First, a wash in laboratory soap and tap water in an ultrasonic bath. All components were then immersed in a 1:1 nitric acid bath for several hours followed by 10 rinses of distilled water. This technique ensured no contamination from the apparatus itself although airborne contamination can have severe effects on surface tension if present. These effects are currently under investigation. The cleaning techniques used for the stage 1 and 2 apparatus were similar, using chromic acid in place of nitric acid. It was thought that the acid may attack the silicone adhesive used to cement the test cell together, therefore the stage 3 test cell was designed.

Preparation of the dyed fluid was undertaken using similarly clean conditions. Fluorescein dye ($C_{20}H_{12}O_5$), 400 mg, and sodium hydroxide (NaOH), 500 mg, were dissolved in 1000 mL of distilled water to produce dyed drops with a specific gravity of 1.001. This small density difference from the test cell fluid is thought to have negligible effects on the experiment discussed here.

The surface tensions of the dyed water and the distilled water within the cell were measured using the capillary rise technique. The addition of the dye did not change the surface tension.

2.2.5. Photography and timing.

Images of the structure were recorded using 35 mm photographs and VHS format

video. The bulk of the data were acquired using 35 mm photographs. These were taken with 400 ASA Ektachrome film using a Nikon F2 and 55 mm Nikkor lens mounted in either the standard or reversed configuration on a bellows extension.

Photographs were taken with the room darkened and camera shutter open, a 15 μ s flash being discharged from a General Radio Type 1540 Strobolume at controlled times after the falling water drop interrupted a .5 mW, He-Ne laser beam (Figure 2.2). The laser beam was declined 5 degrees from horizontal and aimed at the impact site. The stage-3 apparatus used optics to focus the beam to a 30 μ m diameter at the impact site. A photo transistor was situated on the opposite side of the pool to receive the reflected laser light. An interruption of the laser beam by the drop began a counter which would trigger the flash at predetermined delay times.

The times mentioned refer to the interval between the interruption of the laser and the moment that a flash, used to illuminate the phenomenon, is discharged. There is an inherent 300 μ s delay in the timing system's electronic circuit which triggers the flash discharge. There is an error introduced due to the laser beam thickness and from any misalignment of the timing system's optics. This results in some uncertainty if the delay times are to be taken as the time of the event after first contact of the drop with the pool. The uncertainty is $O(1 \text{ ms})$ for the unfocused laser beam (stage-1 and stage-2). This error is unimportant at later times in the event, but during the first 10 ms the geometry of the event changes very rapidly. This error must be considered when comparing photographs taken at similar early times. The focused laser beam reduced the error by an order of magnitude allowing more precise interpretation of the results.

The photographs were taken from three angles to provide understanding of the complex topology of the three-dimensional structure (Figure 2.3). Top and side photographs were taken by adjusting the attitude of the camera mount while axial shots

were taken via a surface-silvered mirror mounted directly below the impact site and at 45 degrees to the free-surface plane. All the photographs have the focal plane parallel to the laser beam that was used to trigger the strobe.

Videotaping was undertaken using a strobe synchronized with a colour video camera using the same optics as the photographic system.

2.3. Experimental Sensitivity

Due to the experiment's extreme sensitivity to initial conditions, great care was required to obtain the conditions under which the drop-created vortex structure studied here would occur. Experiments in which the structure of interest occurred were those conducted within a very small range of the falling drop's We and Fr and the resulting vortex ring's Re , where:

$$Fr = \frac{u^2}{gD} \quad , \quad We = \frac{\rho u^2 D}{\gamma} \quad , \quad Re = \frac{\Gamma}{\nu}$$

This is based on: drop diameter (D), impact velocity of the drop (u), fluid density (ρ), kinematic viscosity (ν), surface tension (γ), and circulation of the vortex ring (Γ). It is surmised that the vortex structure created here will only occur within a narrow window of these parameters. To obtain these conditions and to reproduce this structure required consistently sized drops falling vertically from a carefully adjusted height into a clean pool of water free of any wave motion. Great care had to be exercised to obtain these conditions. The drop height was varied between 34.5 mm and 38.4 mm for the experiments reported. Tuning of the height was accomplished by using video images taken of the structure to give instantaneous feedback as to whether the desired three-dimensional structure occurred or not. On any given day variations over a 1 mm drop-

height range varied the qualitative structure dramatically. It is thought that variation in fluid temperature was primarily responsible for the required height adjustment.

The drop's volume (V) is dependent on the diameter of the tube used to form it and the drop fluid's surface tension. It was found that each hypodermic tube would produce drops of varying volume. This is likely caused by changes in surface tension. Variations in surface tension are to be expected with changes in ambient temperature. The change in volume alters the length scale for the drop's We and Fr . The We also changes directly with temperature due to the variation in the surface tension (γ). As discussed in §2.2.2 oscillations in the drop are induced as it is released from the tip. The drop passes from vertically prolate through spherical to horizontally oblate. It then passes through spherical to vertically prolate completing one period. Lamb (1945) calculates the frequency of an oscillating drop's primary mode which can be rewritten to give the period of oscillation:

$$\tau = \left(\frac{3\pi\rho V}{8\gamma} \right)^{\frac{1}{2}}. \quad (1)$$

It can be seen that variation of the surface tension or drop volume will change the oscillation period.

Photographs of the falling drop taken just prior to impact show the drop's profile to be slightly elliptical with a maximum aspect ratio of 1.1 in the last period before impact. (aspect ratio = $\frac{D_v}{D_h}$, D_v and D_h represent the major and minor axes respectively). Multiple exposure photographs taken of the drop in free-fall reveal that it oscillates throughout the fall with a measured period of 11 ms. Just prior to impact the drop is passing through its vertically prolate phase and is about to become spherical. Figure 2.4 shows the aspect ratio of the drop for the last 14 mm of fall before striking the receiving pool. Due to the higher damping associated with smaller diameter drops

and the increased time of free-fall, the amplitude of the 2.6 mm diameter drop's oscillations decay more than 4.5 mm diameter drops.

The geometry of the free surface during the drop-pool coalescence is altered depending on the drop's oscillation phase at impact. Rodriguez and Mesler (1988) show this for the two extreme cases, that of a fully prolate drop and a fully oblate drop at impact. The free surface geometry is thought to be critical in the production of vorticity as well as the formation of the vortex ring (see §§2.4, 2.5).

It has also been observed that variations of the bath temperature can greatly affect the qualitative vortex structure. This is likely due to the resulting change in the vortex ring's Re number due to the change in kinematic viscosity and the change in the drop's We number due to the change in surface tension. The amount of vorticity within the vortex ring and hence its circulation will also depend on the free surface dynamics as mentioned earlier. This suggests a further dependence of the qualitative vortex structure on the drop's oscillation phase at impact. The method used to estimate the Re is discussed in Appendix 2.

2.4. Experimental Results

The observations reported are based on the examination of several hundred 35 mm photographs taken during the course of these experiments. The photographs accompanying this text have been selected from several different experimental runs for their significance in understanding the evolution of the vortex structure and for their clarity of detail. As mentioned earlier (§2.3), it was necessary to carefully vary the initial conditions before each experiment in order to reproduce the vortex structure. These conditions have been tabulated for each photograph (Table 2.1).

2.4.1. *The falling drop*

The position of the drop centroid vs. time was recorded using multiple exposure photographs to obtain a calculated impact velocity of 80.1 cm/s for a 2.6 mm diameter drop released from 35.5 mm. This measured velocity (u) shows excellent agreement with Pumphrey's result (Pumphrey and Elmore 1990):

$$u = u_T \left[1 - \exp \left(- \frac{2gz}{u_T^2} \right) \right]^{\frac{1}{2}}. \quad (2)$$

Using the terminal velocity (u_T) calculated for a 2.6 mm diameter drop (Dingle and Lee 1973) and subtracting one drop diameter from the measured height for z , the above equation yields 80.11 cm/s, in excellent agreement with the measured value.

2.4.2. *Drop impact and air bubble formation*

At a time of less than 1 ms a small air bubble ($O(100 \mu\text{m})$ diameter) is observed (Plate 2.7). It is located at the leading edge of the impinging drop on the vertical axis of symmetry. The central location of the bubble suggests the drop fluid has made first contact with the pool liquid at latitudes removed from the centre pole. It is concluded that the bubble is formed from a thin, circular sheet of air which becomes trapped between the drop and the free surface. The sheet then quickly collapses into the small spherical bubble under the action of surface tension. The existence of a single bubble on the axis of symmetry has not been reported before.

Esmailizadeh and Mesler (1986) have studied the formation of bubbles by a 2.6 mm diameter drop released from heights below 30 mm. For this case they have shown that the drop impact forms hundreds of small bubbles between 50 and 100 μm diameter.

In the present experiments no bubbles other than the one mentioned were observed regularly. Only occasionally were 2 or 3 bubbles of similar size seen.

While the air bubble is being formed, virtually all of the drop fluid lies above the pool surface and is still approximately spherical. Where the drop and pool coalesce on the interface, a region of high curvature exists which rapidly travels outward until, by 1 ms, the diameter of this region becomes that of the impinging drop (Figure 2.5 (a), (b)). The radial translation of this region is rapid enough to disallow the entrapment of any other air by the impinging drop.

At times less than 1 ms the sides of the drop are now nearly normal to the free surface plane while the trailing edge of the drop retains a hemispherical shape (Plate 2.1). A region of high curvature is visible at the intersection of the near vertical drop wall and the free surface.

Short capillary waves resulting from the impact, with wavelength of $O(.1 \text{ mm})$, are visible on the walls of the exposed drop surface (Plate 2.1). These waves travel toward the top of the drop (Plate 2.2) and have been observed to pinch-off at later times to form a small droplet above the impact crater formed by the free surface. This droplet can then impact upon the centre of the crater. This may account for a small jet-like structure directed vertically down along the vortex ring's axis of symmetry visible in a previously published photograph taken at 10 ms (Peck and Sigurdson 1991). Capillary waves of similar wavelength to those seen on the drop appear on the free surface of the pool and travel radially away from the impact site.

After 1 ms the hemispherical trailing edge of the impinging drop begins to collapse into the pool. By 7.5 ms an entirely concave-up (with respect to the cell fluid) crater is created in the free surface (Plates 2.8, 2.9). The shape of the free surface impact crater is shown in Figure 2.5 for the first 20 ms.

It is known that the crater formed by a similar size water drop impacting with twice the velocity can pinch-off near the deepest point of the crater to form an air bubble. Oguz and Prosperetti (1990) have simulated this event numerically and verified these results with experimental data. They also include an analysis which gives a lower bound of We and Fr for this type of bubble formation. The We and Fr in the present experiments lie below the bounds for the pinch-off. It can be seen in the present data that at the deepest point of crater penetration, which occurs at $7 \text{ ms} \pm .5 \text{ ms}$, there is no pinch off and no further air bubbles are formed.

2.4.3. Birth of the vortex structure

When examining the accompanying photographs it is important not to infer the presence of vorticity by the mere presence of dyed fluid but by considering how the dyed fluid is being convected. Theoretical aspects of vorticity production will be discussed in 2.5 and offer an approach to estimating where the vorticity originates. It is interesting to note that while not all the dyed fluid becomes vortical most does appear to become trapped within the streamlines of the various vortex dipoles within the structure. If a region of initially rotational dyed fluid is considered, from which dye and vorticity are diffusing, it can be shown that the presence of this dyed fluid will indicate the presence of vorticity (see appendix 3 for a more complete discussion). The elapsed time of the event studied is less than 100 ms which limits the vorticity diffusion length ($\sqrt{4\nu t}$, where ν is $.01 \text{ cm}^2/\text{s}$) to .06 cm.

It will now be useful to define what is meant by a vortex ring. For this study the terminology of Glezer and Coles (1990) will be used. The vortex ring will be defined as "an axially symmetric spheroidal volume of fluid whose internal mean vorticity lies entirely in the azimuthal direction". Reference is also made to the vortex ring's core.

This is a region of highly concentrated vorticity which lies along an internal azimuth of the vortex ring forming a toroidal vortex-tube.

At 7.5 ms (Plate 2.9) an axisymmetric distribution of dyed fluid lies below the lower portion of the free surface impact crater. The circumference of the dyed fluid indicates the presence of vorticity which is beginning to roll-up. The vorticity is aligned along azimuths of the impact crater in the form of circular vortex-filaments (a single filament would have a positive impulse where the impulse is as defined in §2.5 and the positive direction is assumed downward). The sign of the vorticity is such that if a single filament were considered in the absence of the free surface it would convect downward under its self-induction. The roll-up continues and by 10 ms (Plate 2.10) a clearly defined toroid of dyed fluid lies next to the free surface near the bottom of the impact crater. Photographs do not show whether a single concentrated core has been formed within the toroid or if there is a broad distribution of vorticity. The vorticity within this toroid will form the primary vortex ring's core.

Plate 2.10 also shows small lobe-like structures which emerge from where the trailing edge of the vortex ring is closest to the free surface. The lobes appear to consist of vortex-filaments which have become unstable during the roll-up process and are hairpin shaped.

By 13 ms the primary ring has separated from the now reversing free surface impact crater (Plate 2.11). The centre of the retracting crater becomes concave-down. The region joining the concave-up and concave-down portions of the crater form an area of high curvature which travels radially outward. Vortex-filaments which would have a negative impulse in the absence of the free surface are successively produced as the area of highest curvature travels over dyed fluid left at the interface. The presence of

this vorticity is indicated by the appearance of a series of concentric rings along the free surface within the concave down portion of the impact crater.

It is surmised that these vortex-filaments coalesce to form the two concentric rings of vorticity observed in Plates 2.5 and 2.6. The smaller diameter (inner) ring is located farther from the free surface than the larger (outer) ring. These "base rings" interact with their images and move radially outward, increasing their diameter. It is from this observation that the sense of the vorticity within the base ring was inferred. This configuration appears to be a stable arrangement in the sense that the rings apparently expand radially at approximately the same rate showing no tendency to leap-frog. These rings later exhibit an azimuthal instability which will be described further in §2.5.

The reversing crater rises only marginally above the free surface and no vertical jet is formed (Figure 2.5 (e), (f)). The parameters for jet formation have been extensively studied and it is well known that drops of this We and Fr are not expected to splash. For a complete discussion of these parameters see Prosperetti (1990).

2.4.4. *The onset of instability*

As the primary vortex ring leaves the free surface the outer diameter of the dyed fluid decreases. It can be seen that this diameter undergoes a decrease until it is 1.5 diameters away from the undisturbed free surface. The primary causes of the diameter reduction are thought to be image effects and the interaction with the unsteady free surface.

The diameter reduction compresses the vortex-filaments along their azimuth. It is during this azimuthal compression that an instability begins to appear within the primary vortex ring. Axial photographs at 14 ms (Plate 2.3) show the first signs of a periodic azimuthal secondary structure at the inner diameter of the toroid. The wave

number (k) on the inner diameter of the toroidal distribution of dyed fluid is observed to be 28 at 14 ms. The wave number has been observed to decrease to 3, 4 or 5 by 19 ms (Plate 2.4). This instability appears to be a series of $2k$ vortex-tubes, alternating in sense, and wrapped around the primary vortex ring's core (Plates 2.12, 2.13). The tubes form k counter-rotating vortex pairs centred on azimuthal planes around the vortex ring's axis of symmetry. The sign of the vortex-tubes in each pair are such that under mutual self-induction the pairs will move radially away from the centre of the core (Figure 2.6.(a), 2.6.(b)). The pairs begin to escape the trapped orbits of the primary vortex ring after 25 ms (Plate 2.14). The escape produces k hairpin vortices or "petals". After the petals escape the vortex ring they begin to curl away from the vertical central axis under the self-induction of the constituent filaments (Plate 2.15). By 65 ms after impact the petals are virtually stationary (Plate 2.16).

The number of petals "shed" has been observed to vary from three to five. The azimuthal position of these petals show remarkable symmetry being equally placed at $2\pi/k$ positions about the ring. This is clearly visible in Plates 2.5 and 2.6 which show three and four shed petals respectively.

2.4.5. Relaminarization and phase lock

After the petals have been shed ($t > 65$ ms) the primary vortex ring is relaminarized and no further instabilities are observed (Plate 2.16). Estimates of the vortex ring Re range from 400 to 1300 which corresponds to the known range of laminar rings. The method used to estimate the Re is discussed in Appendix 2.

As the primary ring moves away from the surface, a "stalk" is left behind along the central axis of travel which is normal to the free surface. The stalk is thought to be formed from a delicate structure of vortex pairs which extend from the primary ring to

the free surface. At the free surface, the vortex pairs diverge from each other radially outward to the inner base ring forming a spoke and wheel structure. Where a spoke meets the inner base ring a concentration of dye at the intersection suggests that this pair might be wrapped around the inner base ring.

It is observed that the number and azimuthal positions of the spokes corresponds with the number and azimuthal positions of the shed petals. These positions also correspond with the vertices of an instability which grows on the base rings. This correspondence suggests an azimuthal phase lock within the structure. The phase lock is not completely understood, but may be born at early times ($t < 10$ ms) when the entire vortex structure is still close together and near the free surface.

The origin of the stalk is conjectured to be as follows. When the free surface crater is reversing, filaments from the primary ring may become captured within the orbits of the forming base ring. If considering an individual circular vortex-filament, at some azimuthal locations it would be caught in the base ring, at adjacent locations it would be caught in the primary ring. This would result in the severely stretched vortex pairs that appear in the stalk when at later times the primary ring and base ring convect away from each other. The stalk is therefore modelled as one closed line vortex extending back and forth between the primary ring and the inner base ring.

2.5. Discussion

2.5.1. Vorticity generation

To understand the vortex structure created by the impact of a water drop, the birth of the vorticity must be understood as well as its evolution. The means by which

the necessary torques are generated to produce the vorticity associated with this problem are not well understood. For the general case of vorticity production at a free surface it is thought that a baroclinic torque is generated due to gradients in pressure tangential to the free surface acting on the discontinuous density gradient across it. Batchelor (1967) provides a kinematic condition for the jump in vorticity ($\Delta\omega$) required across the boundary layer which forms at a free surface. For the case of a wave moving at steady velocity this condition can be written as:

$$\Delta\omega = 2\kappa q^* \quad (3)$$

The presence of surface curvature (κ) and a tangential fluid velocity (q) requires this vortical layer to satisfy the shear-free boundary condition. While this is for the steady case, Ohring and Lugt (1990) show that a qualitative understanding of the magnitude and sign of vorticity produced can be deduced from examination of the surface curvature and the velocity field in unsteady problems.

For the subsequent discussion it will be useful to define the impulse \mathbf{I} of the vorticity distribution in an infinite fluid:

$$\mathbf{I} = \frac{1}{2} \rho \int_V \mathbf{r} \wedge \boldsymbol{\omega} dV \quad (4)$$

In the absence of boundaries the impulse is a time invariant quantity, even in the presence of viscosity (Batchelor 1967). Evaluating this integral for a single circular vortex-filament yields an impulse parallel to the filament's axis of symmetry and in the direction of the filament's travel under its self-induction. For the present case the impulse of the primary vortex ring is directed vertically down and will be referred to as positive.

*This equation is derived and discussed further in Appendix 3.

The vorticity with positive impulse, visible by 7.5 ms (Plate 2.9) has been created in the time since first contact of the drop with the pool. It is proposed that vorticity is generated in the following manner. The penetrating drop produces a velocity tangential to the free surface in the region of high curvature where the drop and pool coalesce. Equation 3 indicates that vorticity must be produced to satisfy this condition. Initially the region of highest curvature will be near the central axis of the impact crater as the drop and pool first coalesce. At a time of less than 1 ms the location of greatest curvature has travelled radially outward to approximately the radius of the drop. The position of the maximum curvature then moves radially inward along the top surface of the drop (now coalesced) until it reaches the central axis and a completely concave-up crater forms. Throughout the formation of the concave-up crater the tangential fluid velocity will be radially outward with respect to the area of maximum curvature. In this way the vorticity associated with positive impulse is successively produced as the area of curvature travels back and forth. The magnitude of the tangential velocity is unknown at each time during the formation of the concave up crater. As a result the initial distribution of vorticity within the resulting vortex sheet cannot be estimated.

Similarly, circular vortex-filaments with negative impulse appear in the reversing impact crater. The tangential flow is now radially inward and vorticity is created at the region of high curvature joining the concave-up impact crater and the concave down reversing crater. The boundary layer appears to separate on the inner edge of the reversing crater forming a series of concentric rings as the crater enlarges. Eventually these rings coalesce into two or three base rings which interact with their images and convect radially outward. This increases the circumference of the filaments intensifying the vorticity within the base rings.

2.5.2. Vortex model

The proposed vortex structure, modelled with 5 closed line vortices, is shown in Figure 2.7. This is representative of the structure which occurs at times of 50 to 65 ms and is thought to show the greatest similarity with the above-ground atomic blast.

The most dominant and robust feature in the structure is the primary vortex ring core modelled here as a closed, circular line vortex of strength Γ_1 . At the times mentioned ($50 < t < 65$ ms) there are no azimuthal waves along the core axis and the finer scale structure visible at earlier times is absent.

In the wake of the primary vortex ring are the petals, modelled here as a single continuous line vortex closing on itself. The petals join the primary vortex ring at its trailing edge very near the central axis of symmetry. The dyed fluid forming the petals is indeed vortical. This is confirmed by observations of the very tips of the petals occasionally pinching off and forming small vortex rings which then proceed to convect away from the central axis at oblique angles. This supports the hypothesis that the origin of the petals is a series of vortex pairs wrapped around the primary vortex ring core visible in the data at 15 ms. In this way vorticity is transported out of the primary ring into the wake.

As discussed earlier the impulse of the system \mathbf{I} is invariant with time in the absence of external forces. For the case of the impacting drop the impulse lies only in the vertically down direction. Due to the axisymmetry no net impulse lies in the radial direction initially and its invariance forces the radial component of \mathbf{I} to vanish for all time. If an individual petal is considered, some of its impulse must lie in the radial direction.

(Figure 2.8). There is no other net radial impulse within the structure since the primary vortex ring continues vertically downward and the symmetry of the base rings contributes

no radial impulse. Since the radial component of \mathbf{I} must vanish the sum of this portion of the k petals' impulse must be zero. Modelling the k petals as a continuous line vortex, it follows that a distribution of topologically similar petals at equiangular azimuthal positions is sufficient to satisfy the condition of zero radial impulse.

Along the central axis of the structure the stalk connects the primary ring with the base rings (Figure 2.9). This structure, like the petals, is modeled with a single highly convoluted, closed line vortex. At the primary vortex ring, portions of this line vortex are trapped within the primary vortex ring's closed streamlines. From the primary vortex ring the portions of the line vortex which form the stalk travel along the vertical axis of symmetry to the base of the structure. At the free surface the pairs which form the stalk extend radially outward, terminating at the inner base ring. Here their tips are caught within the closed streamlines formed by the inner base ring and its image. If an azimuthal plane is positioned normal to the plane free surface in such a way as to cut through a radial pair it can be seen that the pairs which form the petals will be bisected by it. This represents the azimuthal phase lock within the structure.

It is likely that the fluid within the stalk becomes dynamically inactive quite quickly. It has been shown that the cancellation of vorticity is enhanced in the presence of axial strain (Schatzle 1987). With reference to Figure 2.8 it can be seen that the sections of the line vortex which comprise the stalk are in close proximity to one another. In the two-dimensional plane the sign of each portion of the stalk is opposite to that of its neighbour and is undergoing a severe out of plane strain; thus the conditions for enhanced vorticity cancellation are fulfilled.

The time scale suggested by Schatzle for the cancellation to occur through a core of radius δ undergoing a strain ϵ is:

$$t_c \approx \frac{2\delta}{\sqrt{\epsilon v}} \quad (5)$$

From photographic measurements ϵ was estimated to be $O(30 \text{ s}^{-1})$ and δ as 10^{-2} cm . This gives a cancellation timescale t_c of $O(35 \text{ ms})$. After the vorticity is cancelled throughout the core the line vortex will have to reconnect with itself thus allowing the stalk to separate from the primary vortex ring.

There is also an outer base ring. This larger diameter ring lies closer to the free surface than the inner ring. The inner and outer rings are each modeled with a single line vortex of opposite impulse to the primary ring. Both the inner and outer rings become unstable with time. The instability takes the form of k large amplitude waves in the plane of the undisturbed free surface. It is noteworthy that the vertices of the perturbed rings correspond to the azimuthal position of the radial pairs.

2.5.3. *Similarity to other flow topologies*

The vortex structure proposed here for an impacting water drop is topologically quite similar to other flows: the separation bubble on a blunt flat plate and the mushroom cloud from an above-ground atomic blast. It was knowledge of the hairpin vortices which allowed Professor Sigurdson to identify the hairpins in the petals of the present structure. The separation bubble structure has been described by Sigurdson and Roshko (1984), Sigurdson (1986,1992) and Kiya (1989). Both it and the present structure have a region of trapped orbits. Three-dimensionalization of the line vortices creates a situation where part of a line vortex "escapes" to form a hairpin, and part remains within the trapped region.

The topological similarity of the present structure with the atomic blast is stronger than with the separation bubble. It is thought that the reason for this is the similarity in

the initial geometry of the vorticity generation (Sigurdson 1991). Now that more information is available for the present structure, this comparison will be the subject of another paper.

The origin of the petals is thought to be the finer scale structure observed at 14 ms in the primary vortex ring (Plate 2.3) which grows into a series of vortex pairs wrapped around the primary vortex ring's core. A similar structure has been observed by Glezer and Coles (1990) in orifice-discharge produced vortex rings. In their study of turbulent vortex rings the existence of a series of small vortex-tubes, alternating in sense, wrapped around the primary core was observed. From the published photographs it seems that these tubes are organized in counter-rotating pairs producing the same geometry as observed for the water drop produced vortex rings at 15 ms.

Part of the value in studying the present structure is that it offers a simplified version of some of the vortex dynamics which may occur in these other flows.

References for Chapter 2

- Batchelor G.K. 1967 *An Introduction to Fluid Dynamics*. Cambridge University Press.
- Bernal L.P. and Kwon J.T. 1989 Vortex ring dynamics at a free surface. *Phys. Fluids A* **1**, 449-451.
- Chapman D.S. and Critchlow P.R. 1967 Formation of vortex rings from falling drops. *J. Fluid Mech.* **29**, 177-185.
- Dingle A.N. and Lee Y. 1972 Terminal fall speeds of raindrops. *J. Appl. Met.* **11**, 877-879.
- Esmailizadeh L. and Mesler R. 1986 Bubble entrainment with drops. *J. Colloid Interface Sci.* **110**, 561-574.
- Glezer A. and Coles D. 1990 An experimental study of a turbulent vortex ring. *J. Fluid Mech.* **211**, 243-283.
- Kiya M. 1989 Separation bubbles, in: *Theoretical and Applied Mechanics*. P. Germain, M. Piau and D. Caillerie (eds.), Elsevier Science Publishers, B.V. (North Holland) IUTAM, 173.
- Keedy H.F. 1967 Vortex rings formed by free surface interactions. Ph.D. thesis, University of Michigan.
- Lamb H. 1945 *Hydrodynamics*. (6th edition), Dover Press, New York.
- Longuet-Higgins M.S. 1953 Mass transport in waves. *Phil. Trans. R. Soc. Lond. A* **245**, 535-581.
- Longuet-Higgins M.S. 1992 Capillary rollers and bores. *J. Fluid Mech.* **240**, 659-679.
- Maxworthy T. 1972 The structure and stability of vortex rings. *J. Fluid Mech.* **51**, 15-32.
- Maxworthy T. 1974 Turbulent vortex rings. *J. Fluid Mech.* **64**, 227-239.
- Oguz H. and Prosperetti A. 1990 Bubble entrainment by the impact of drops on a liquid surface. *J. Fluid Mech.* **219**, 143-179.
- Ohring S. and Lugt H.J. 1990 Interaction of a viscous vortex pair with a free surface. *J. Fluid Mech.* **227**, 47-73.
- Okabe J. and Inoue S. 1961 The generation of vortex rings, II. *Rept. Res. Inst. Appl. Mech.* **9**, 147-156.

- Peck B.J. and Sigurdson L.W. 1991 Gallery of Fluid Motion: Impacting Water Drop. *Phys. Fluids A* 3, Helen Reed (ed.), 2032.
- Pumphrey H.C. and Elmore P.A. 1990 The entrainment of bubbles by drop impacts. *J. Fluid Mech.* 220, 539-567.
- Rodriguez F. and Mesler R. 1988 The penetration of drop-formed vortex rings into pools of liquid. *J. Colloid Interface Sci.* 121, 121-129.
- Rogers W.B. 1858 On the formation of rotating rings by air and liquids under certain conditions of discharge. *Am. J. Sci.* 26, 246-258.
- Ryskin G. and Leal L.G. 1984a Numerical solutions of free-boundary problems in fluid mechanics. Part 1. *J. Fluid Mech.* 148, 1-18.
- Ryskin G. and Leal L.G. 1984b Numerical solutions of free-boundary problems in fluid mechanics. Part 2. Buoyancy driven motion of a gas bubble through a quiescent liquid. *J. Fluid Mech.* 148, 19-36.
- Ryskin G. and Leal L.G. 1984c Numerical solutions of free-boundary problems in fluid mechanics. Part 3. Bubble deformation in an axisymmetric straining flow. *J. Fluid Mech.* 148, 37-54.
- Saffman P.G. 1970 The velocity of viscous vortex rings. *Stud. Appl. Math.* 49, 371-380.
- Schatzle P.R. An experimental study of fusion of vortex rings. Ph.D. Thesis, Graduate Aeronautical Laboratories, California Institute of Technology, May 1987.
- Shariff K. and Leonard A. 1992 Vortex rings. *Ann. Rev. Fluid Mech.* 24, 235.
- Sigurdson L.W. and Roshko A. 1984 The large-scale structure of a turbulent reattaching flow. *Bull. Am. Phys. Soc.* 23, 1542.
- Sigurdson L.W. The structure and control of a turbulent reattaching flow. Ph.D. Thesis, Graduate Aeronautical Laboratories, California Institute of Technology, June, 1986.
- Sigurdson L.W. 1991 Gallery of fluid motion: Atom bomb/water drop. *Phys. Fluids A*, 3, Helen Reed (ed.), 2034.
- Sigurdson L.W. and B.J. Peck 1991 The structure created by an impacting water drop. *Bull Am. Phys. Soc.*, 36, 2619.

- Sigurdson L.W. 1992 The three-dimensional structure of a turbulent reattaching flow. (to be submitted).
- Smedley G. and Coles D. 1989 Some transparent immiscible liquid pairs. *J. of Colloid and Interface Science* **1**, 42-60.
- Thomson J.J. and Newall H.F. 1885 On the formation of vortex rings by drops falling into liquids and some other allied phenomena. *Proc. R. Soc. London* **39**, 417-436.
- Trygvasson G., Abdollahi-Alibeik J., Willmarth W.W. and Hirsa A. 1992 Collision of a vortex pair with a free surface. *Phys. Fluids A* **4**, 1215-1229.
- Widnall S.E. and Sullivan J.P. 1973 On the stability of vortex rings. *Proc. R. Soc. Lond. A* **332**, 335-353.
- Widnall S.E., Bliss D.B. and Tsai C.Y. 1974 The instability of short waves on a vortex ring. *J. Fluid Mech* **66**, 35-47.
- Willmarth W.W., Trygvasson G., Hirsa A. and Yu D. 1989 Vortex pair generation and interaction with a free surface. *Phys. Fluids A* **1**, 170-172.

Plate	Apparatus	D (cm)	z (cm)	u (cm/s)	We	Fr
1	Stage 2	.25	3.50	79.6	22	26
2	Stage 2	.25	3.50	79.6	22	26
3	Stage 2	.26	3.50	79.5	23	25
4	Stage 2	.26	3.50	79.5	23	25
5	Stage 2	.26	3.50	79.5	23	25
6	Stage 2	.26	3.50	79.5	23	25
7	Stage 1	.25	3.84	83.6	25	28
8	Stage 1	.25	3.84	83.6	25	28
9	Stage 2	.26	3.55	80.1	23	26
10	Stage 1	.25	3.84	83.6	25	28
11	Stage 2	.26	3.45	78.9	22	25
12	Stage 2	.26	3.50	79.5	23	25
13	Stage 2	.26	3.50	79.5	23	25
14	Stage 2	.25	3.57	80.5	23	26
15	Stage 1	.25	3.84	83.6	25	28
16	Stage 2	.25	3.55	80.2	22	26

Table 2.1. Summary of experimental conditions: D is drop diameter, z is height of hypodermic tube above the free surface and u is the impact velocity of the drop.

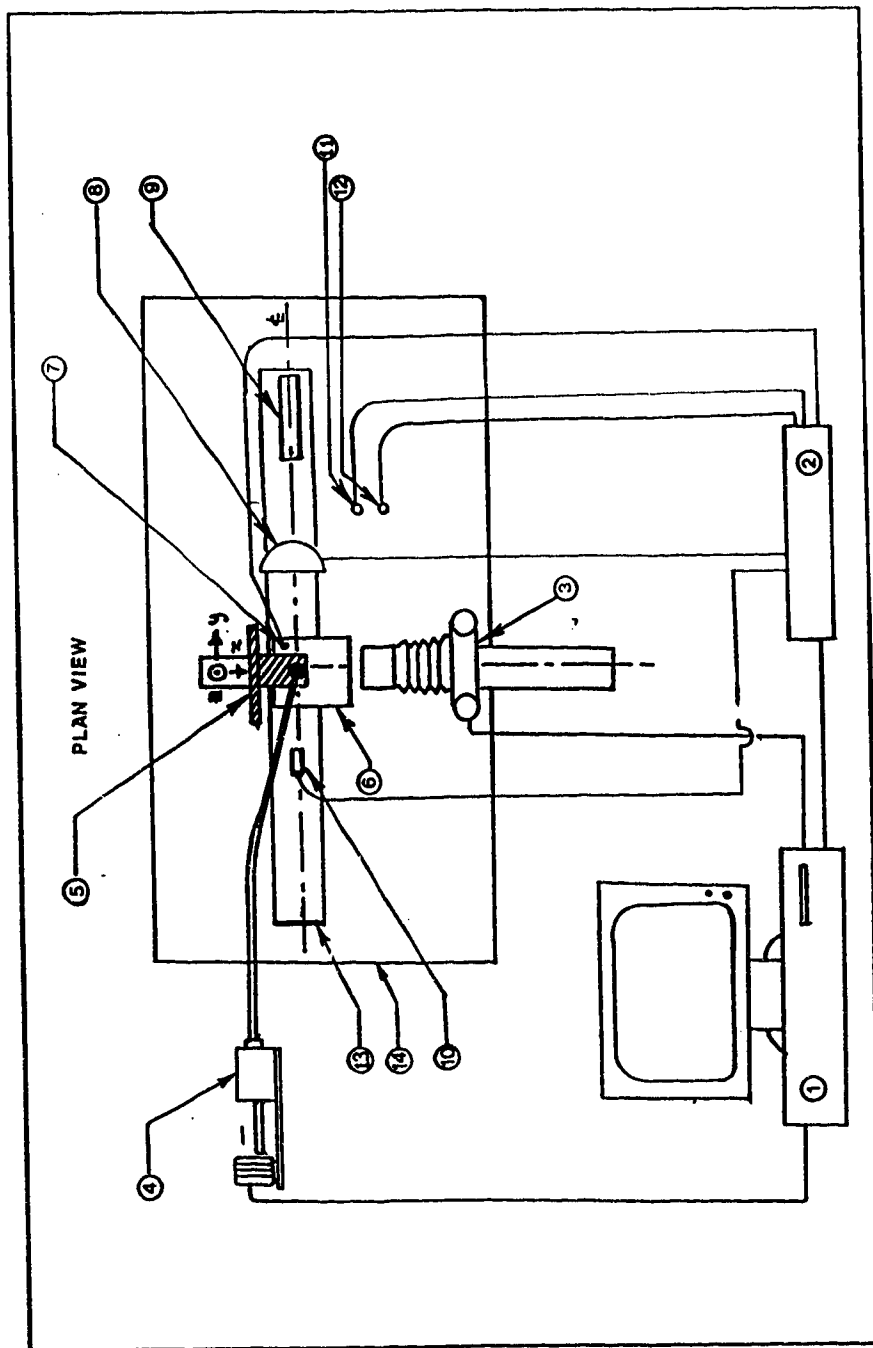


Figure 2.1. Apparatus: (1) personal computer, (2) data acquisition/management board (DA/M), (3) 35 mm camera, (4) stepper-motor driven, precision pump, (5) three-axis traverse and hypodermic tube carrier, (6) test cell, (7) cell temperature probe, (8) strobe, (9) He-Ne triggering laser, (10) photo-transistor to receive laser beam, (11) relative humidity sensor, (12) ambient temperature sensor, (13) optical benches, (14) vibration-isolation table.

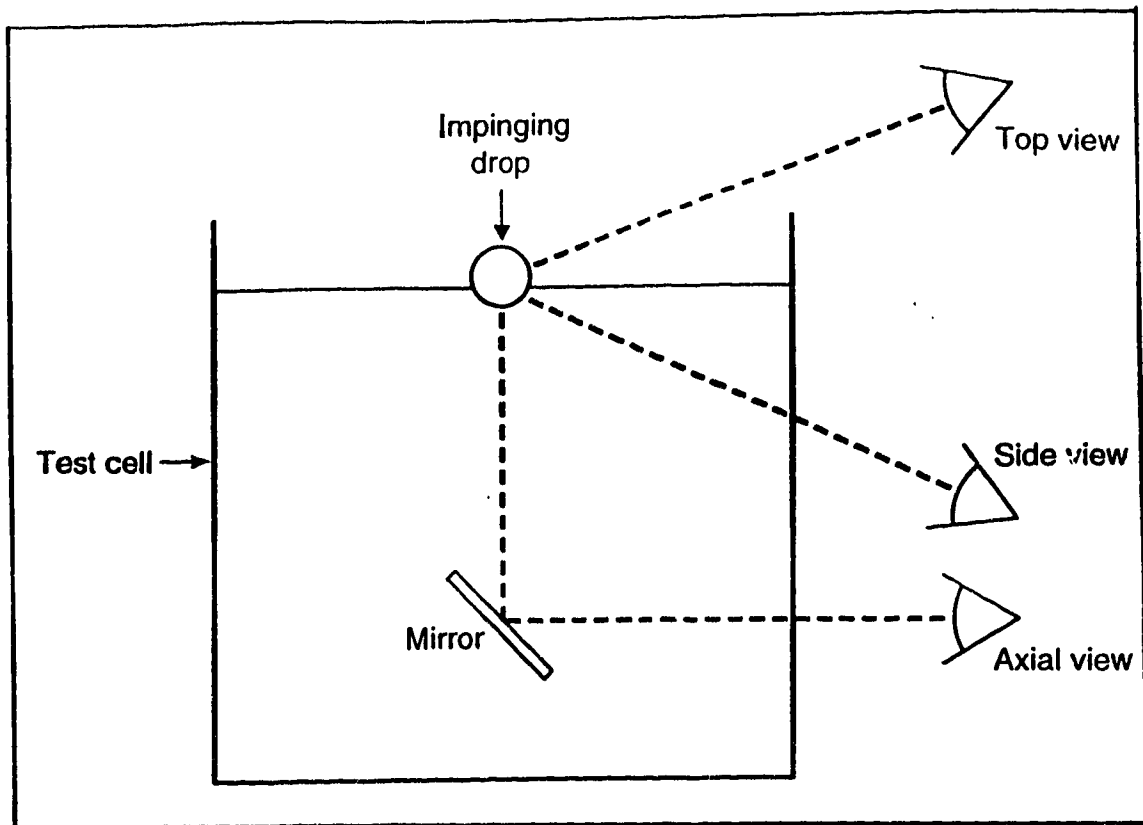


Figure 2.2. Viewing positions, note the mirror mounted at 45° used to obtain axial photographs.

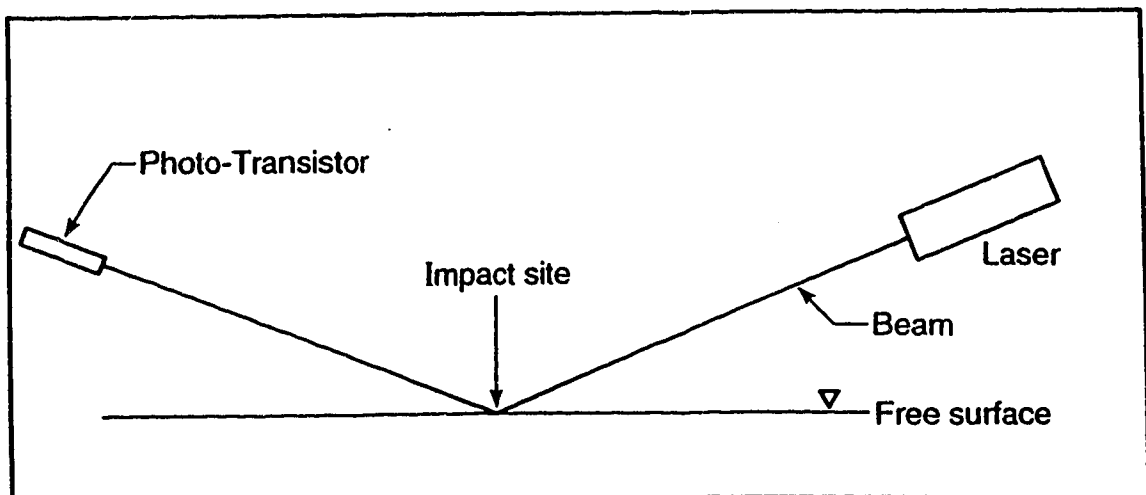


Figure 2.3. Laser optic alignment used to trigger flash discharge.

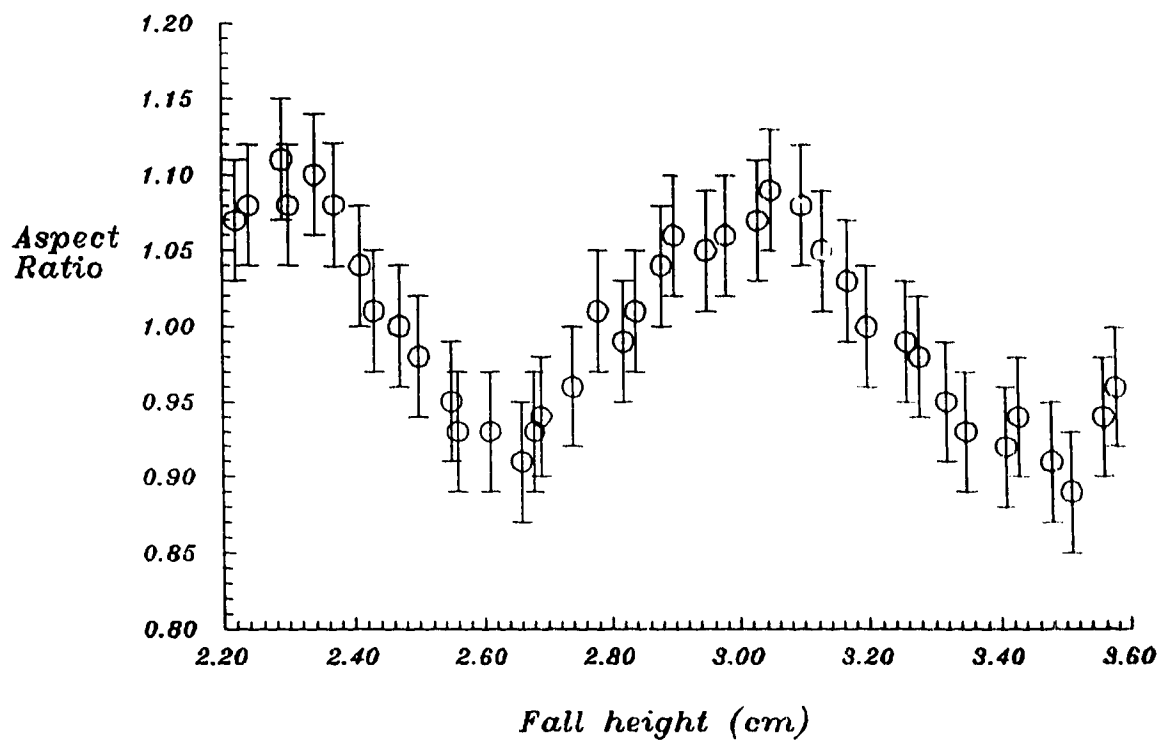


Figure 2.4. The aspect ratio of the 2.6 mm diameter drop in free-fall. It should be noted that in this figure the fall height is the distance from the drop centroid to the tip of the hypodermic tube.

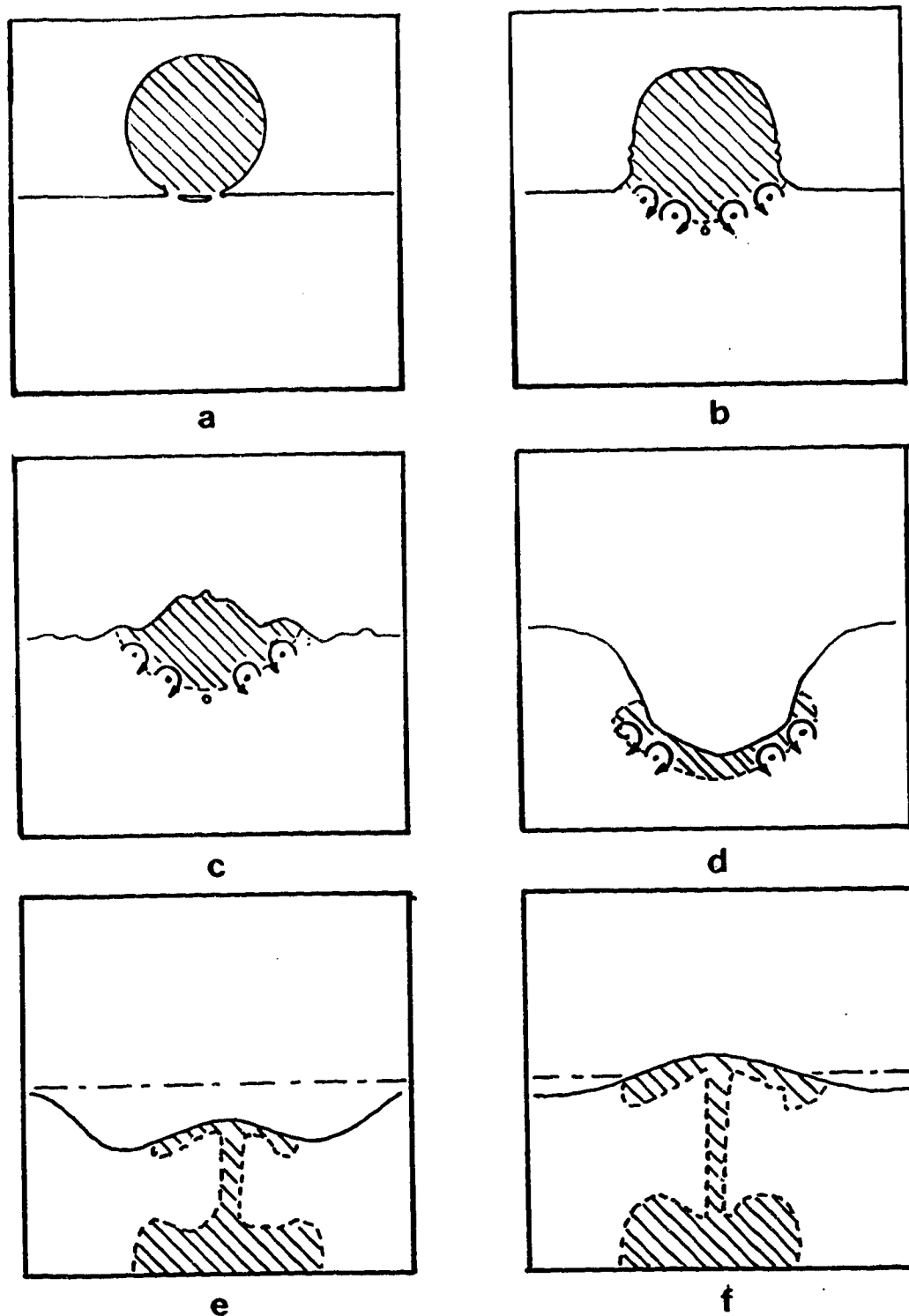


Figure 2.5. Profile of free surface during the first 20 ms after impact. The location of the dyed fluid is shown with the dashed line in (b), (c) and (d). The position of the undisturbed free surface is indicated by the broken line in (e) and (f); (a) and (b) $t < 1$ ms; (c) $t = 2.5$ ms; (d) $t = 7.5$ ms; (e) $t = 15$ ms; (f) $t = 20$ ms. The location of the vorticity is indicated in (b), (c) and (d).

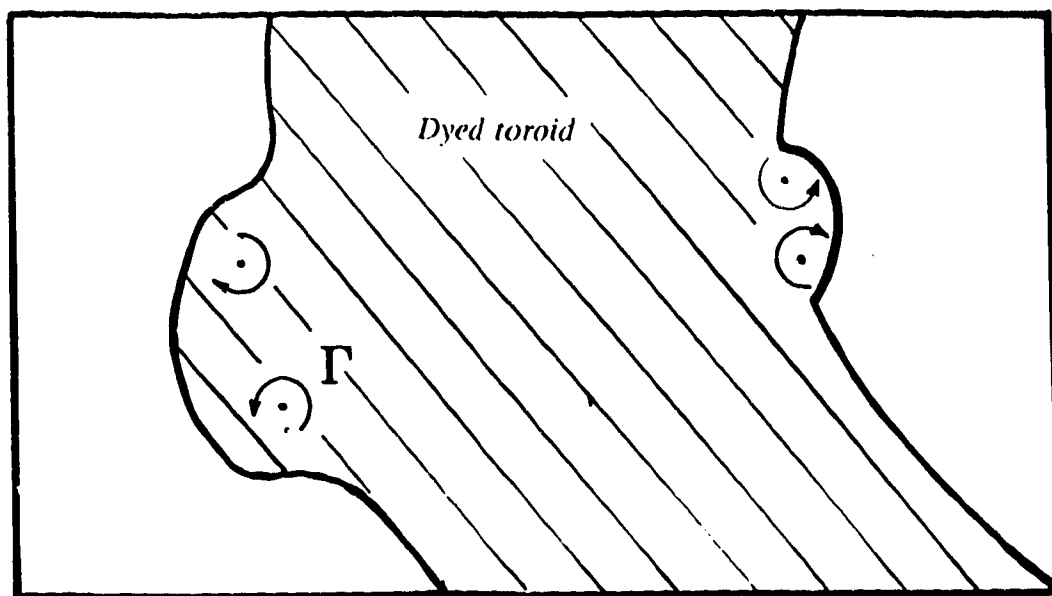


Figure 2.6.(a). A sketch of the secondary structure appearing in the primary vortex ring at $t = 19$ ms. The sketch is taken from plate 2.4. The vortex ring's axis of symmetry is out of the page. The primary vortex ring's core lies within the dyed toroid but its exact position is unknown.

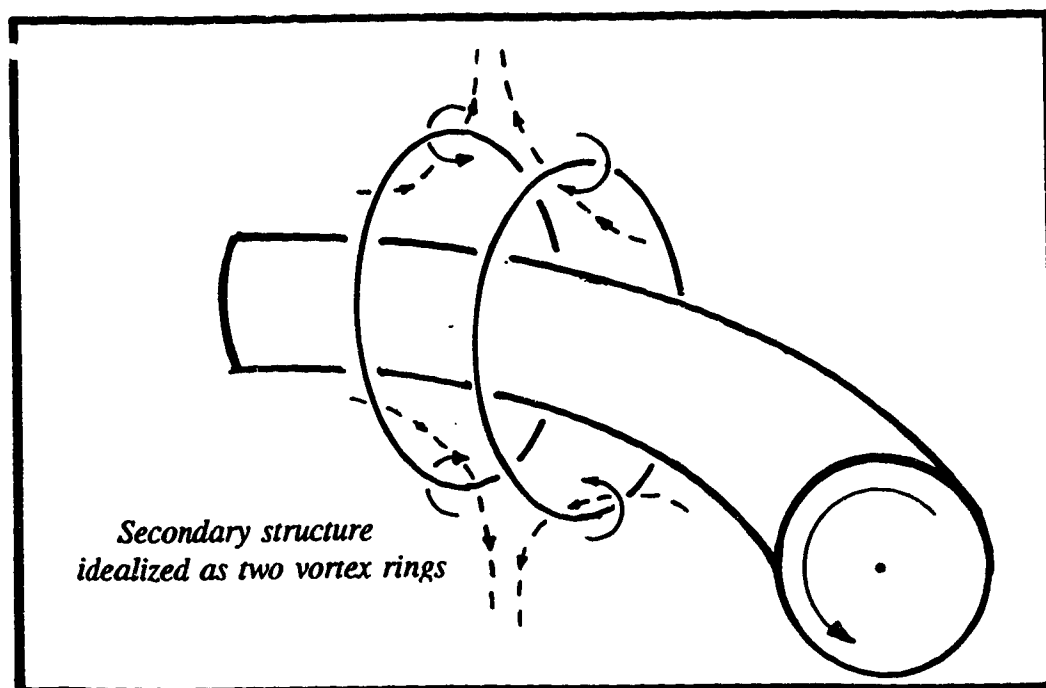


Figure 2.6.(b). Idealized sketch of the secondary structure. The vortex pairs have wrapped around the primary core forming two vortex rings of opposite sense. They convect towards each other and move (locally) radially outward.

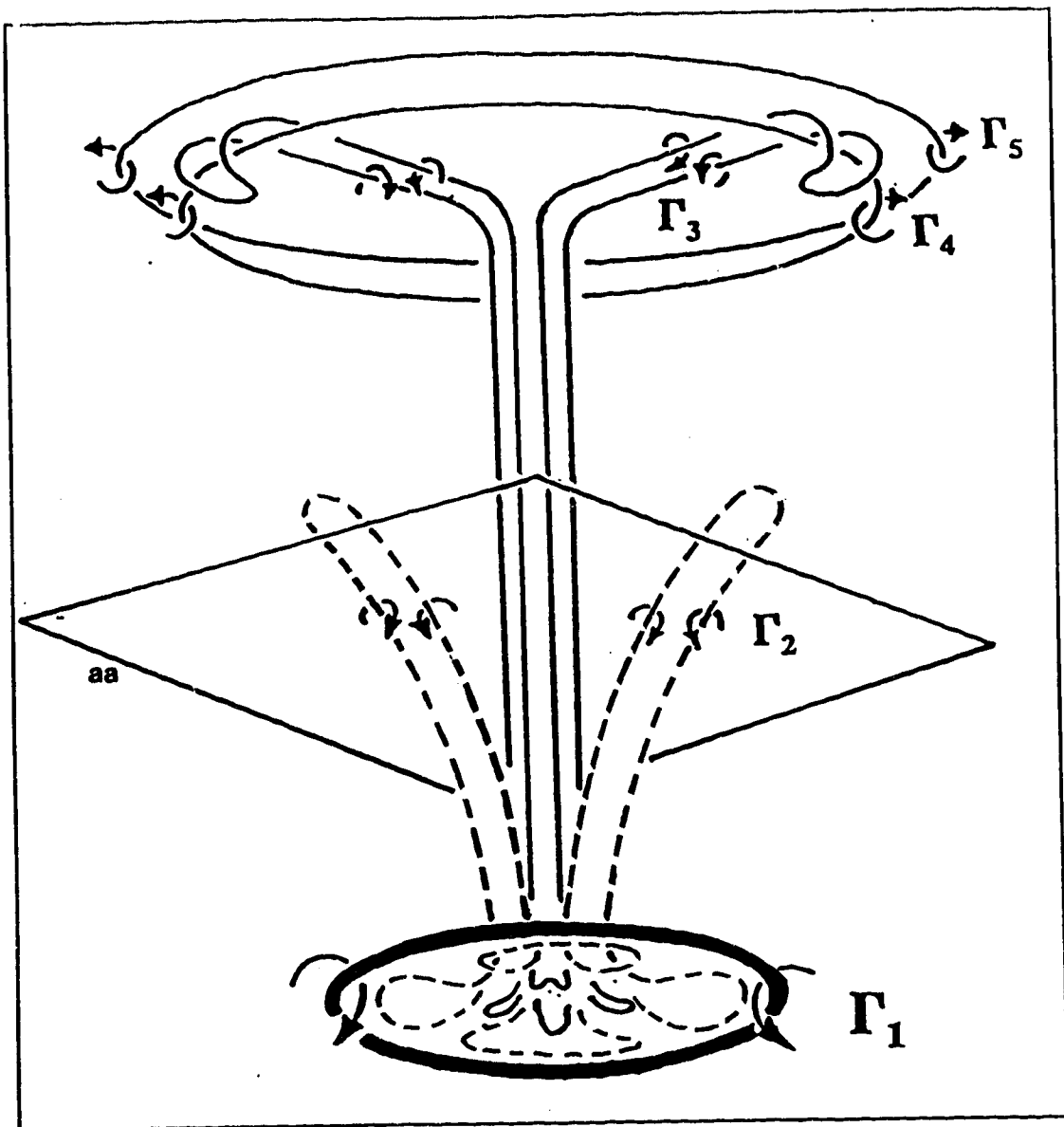


Figure 2.7. The proposed three-dimensional vortex skeleton. The circulations (Γ) associated with each of the five closed line vortices are indicated. Γ_1 corresponds to the primary vortex ring core, Γ_2 the circulation of the line vortex forming the "petals", Γ_3 the "stalk", Γ_4 the inner "base" ring and Γ_5 the outer "base" ring. For clarity only two of the "petals" and two portions of the "stalk" are shown.

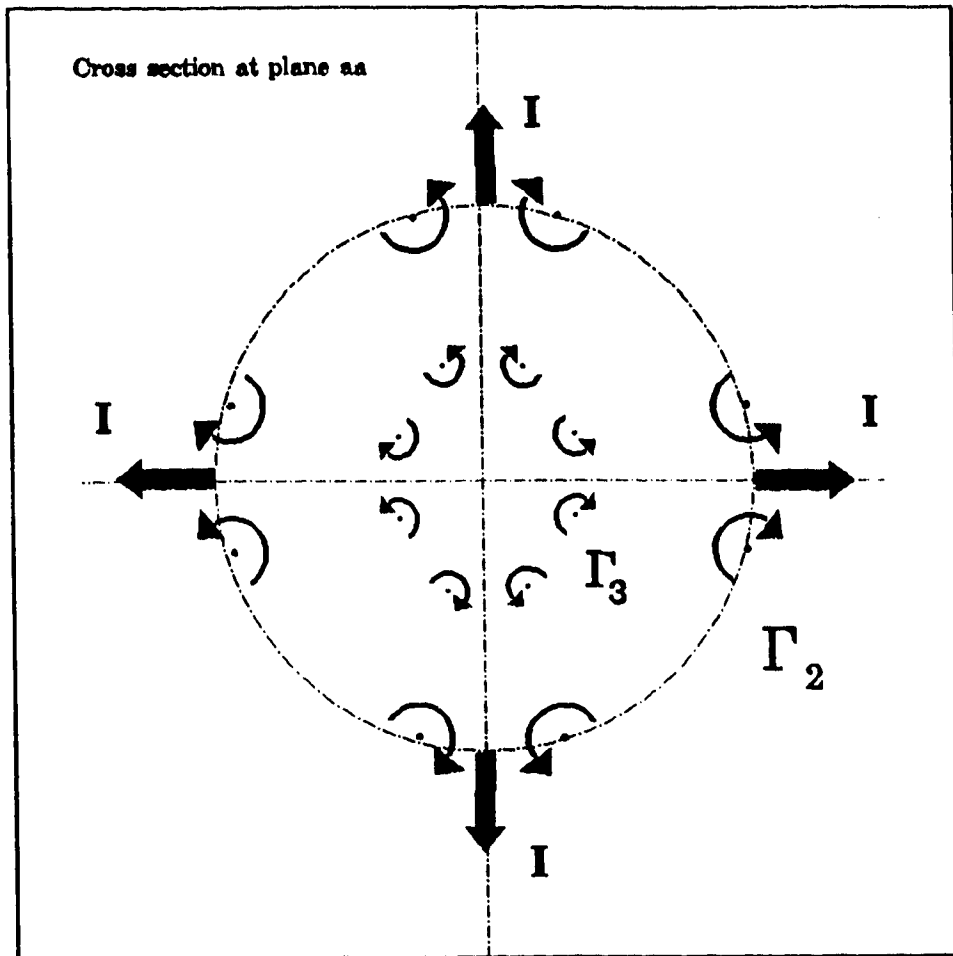


Figure 2.8. Two-dimensional section through the three-dimensional vortex skeleton model at plane aa (see figure 2.7). The outer vortices correspond to the "petals" while the inner vortices correspond to the "stalk". The sense of the circulation is indicated by the arrows.

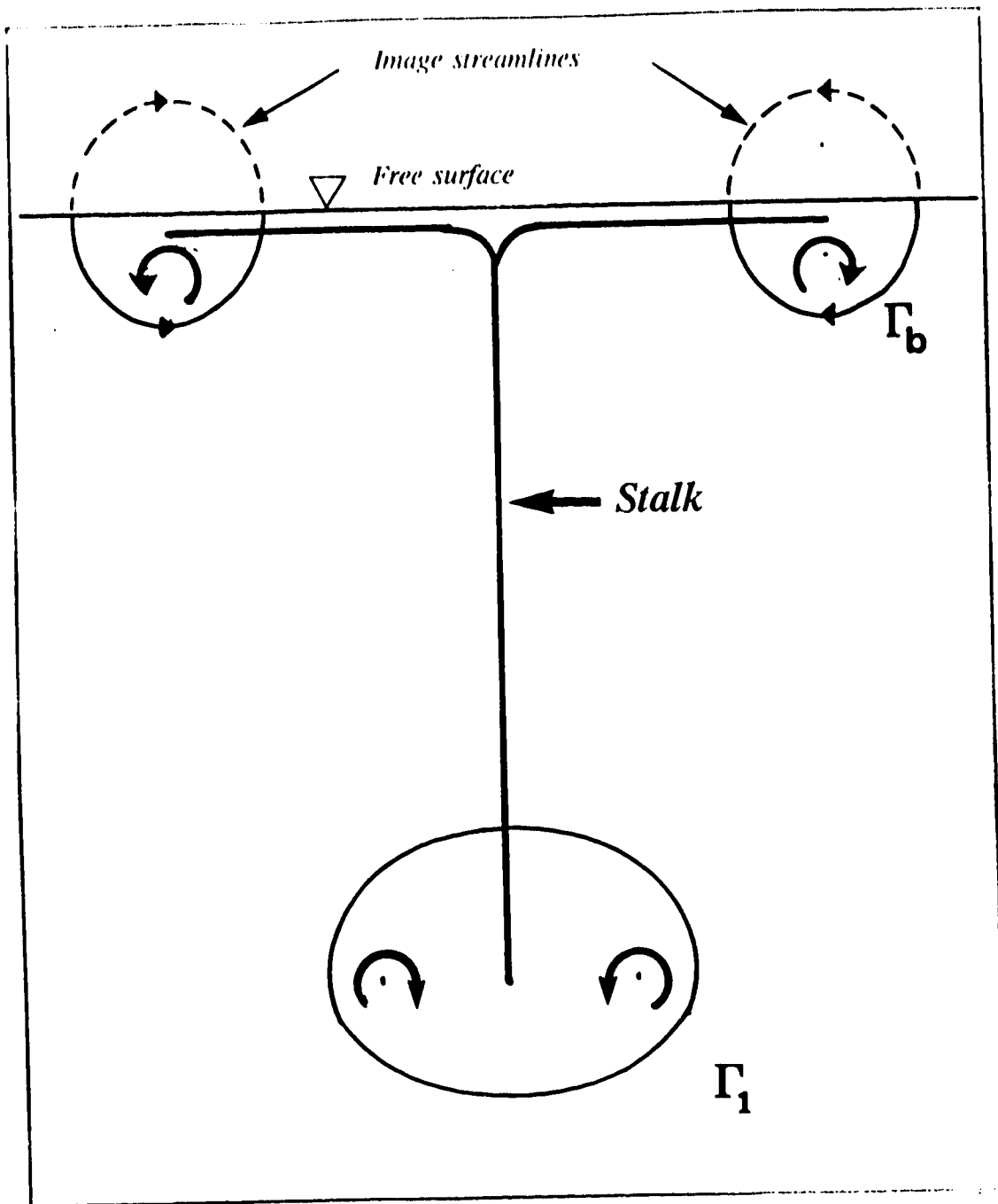


Figure 2.9. The trapped streamlines of the primary vortex ring and the base rings (the image streamlines are indicated with dashed lines). The base rings are idealized here as a single line of vorticity with strength Γ_b .

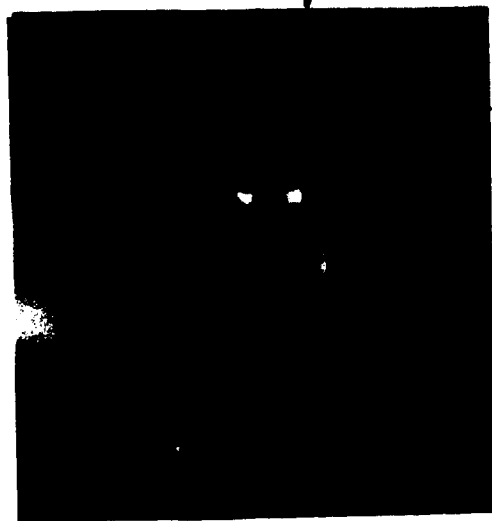


Plate 2.1.
Top view of drop impact, $t < 1$ ms.

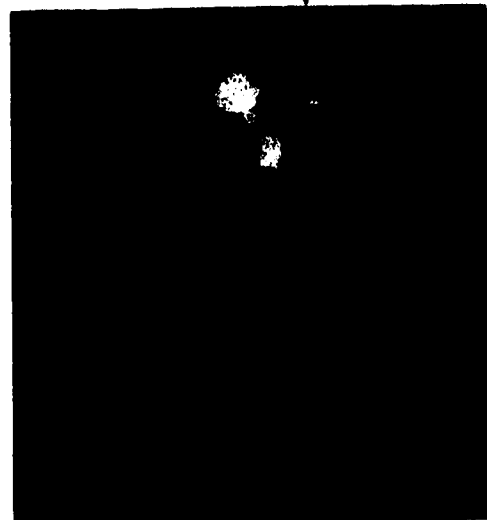


Plate 2.2.
Top view of drop impact, $t = 1.3$ ms.

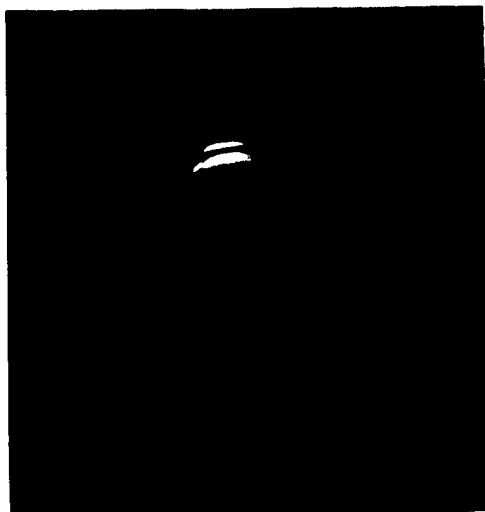


Plate 2.3.
Axial view of drop created
vortex structure, $t = 14$ ms.



Plate 2.4.
Axial view, $t = 19$ ms.

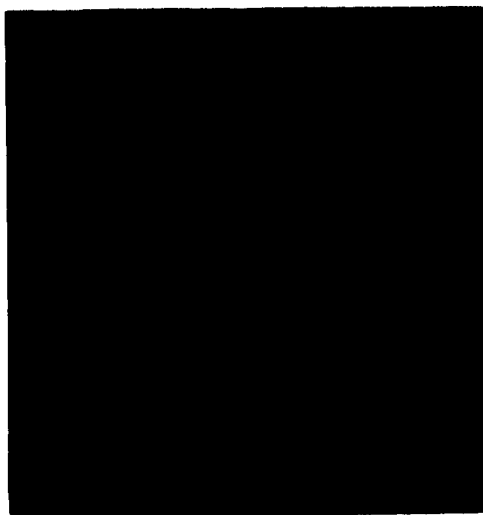


Plate 2.5.
Axial view $k=3$,
 $t = 65$ ms.

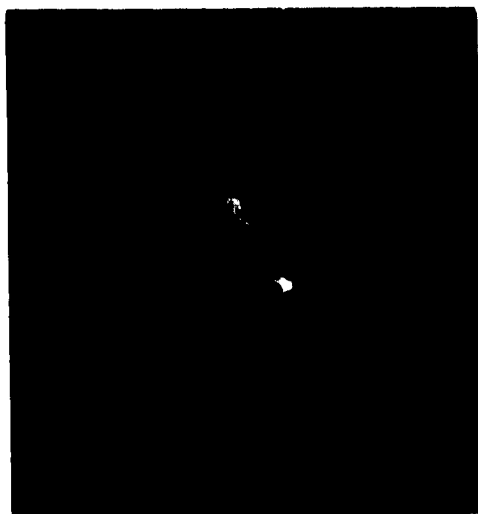


Plate 2.6.
Axial view, $k=4$,
 $t = 65$ ms.

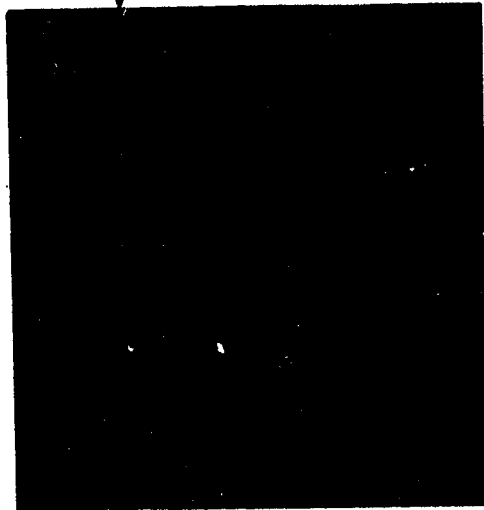


Plate 2.7.
Side view of impinging drop,
 $t < 1$ ms.

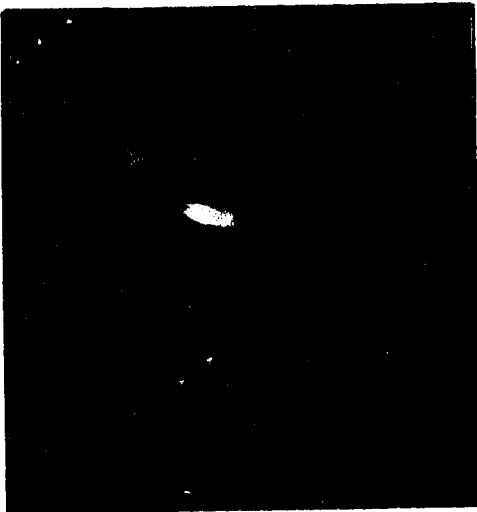


Plate 2.9.
Side view of drop created
vortex structure, $t = 7.5$ ms.

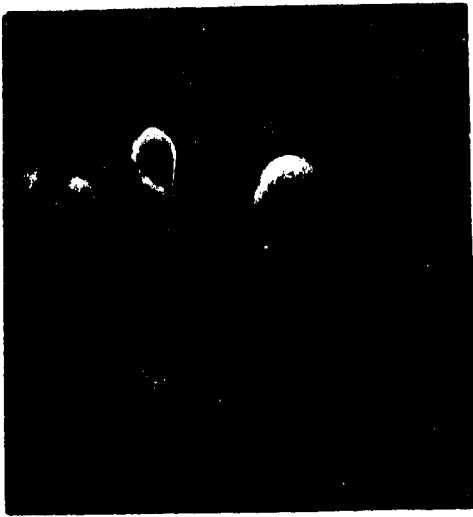


Plate 2.11.
Side view, $t = 13$ ms.

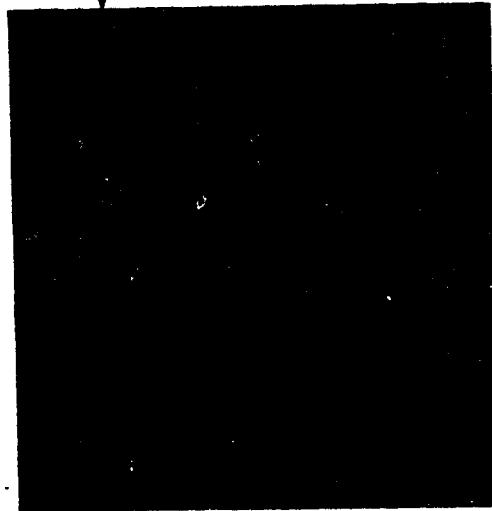


Plate 2.8.
Side view, $t = 2.5$ ms.



Plate 2.10.
Side view, $t = 9.0$ ms.



Plate 2.12.
Side view, $t = 16$ ms.



Plate 2.14
Side view, $t=30$ ms.

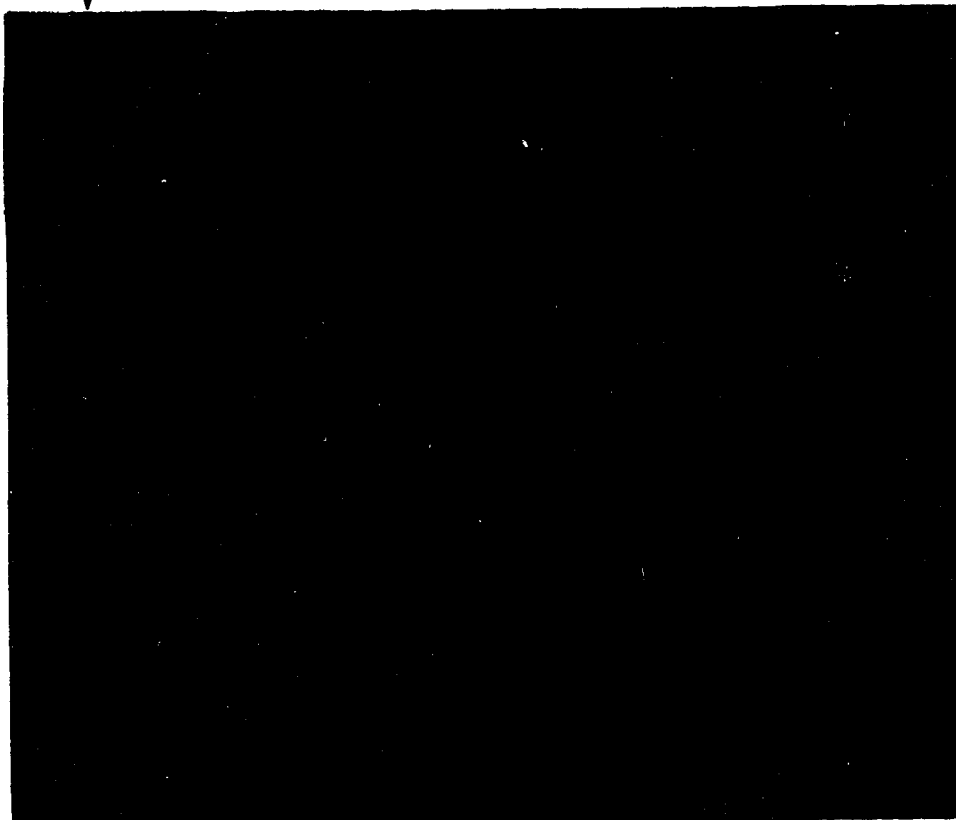


Plate 2.13.
Side view, $t=20$ ms.

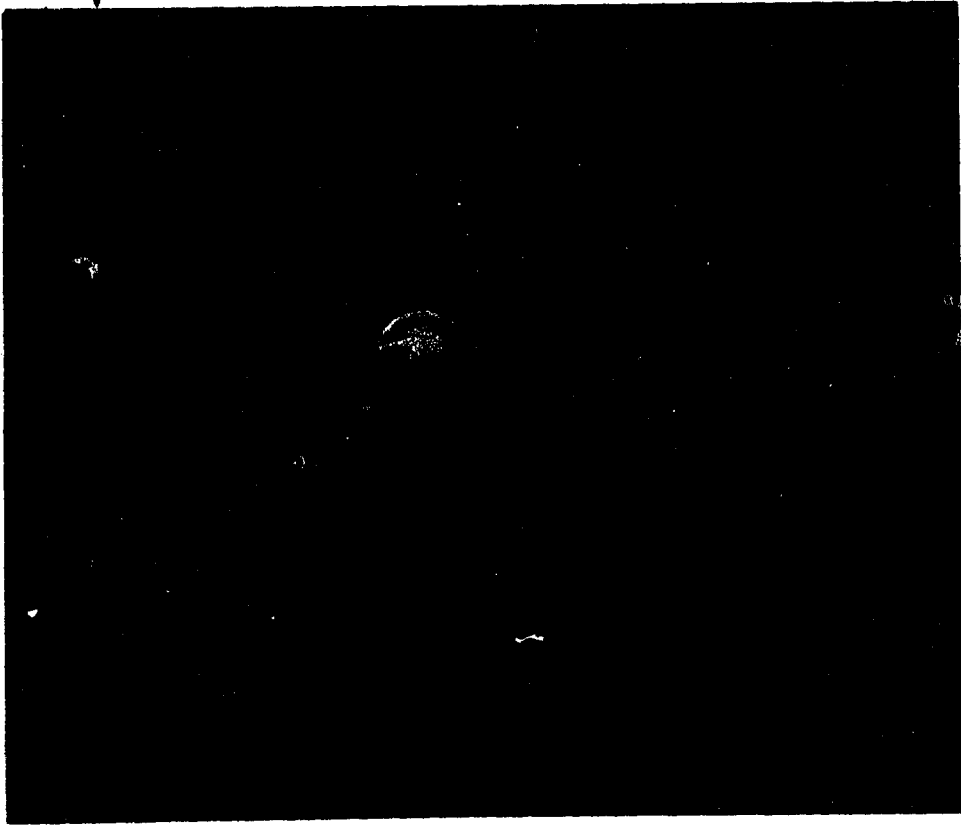


Plate 2.15
Side view, $t = 65$ ms.

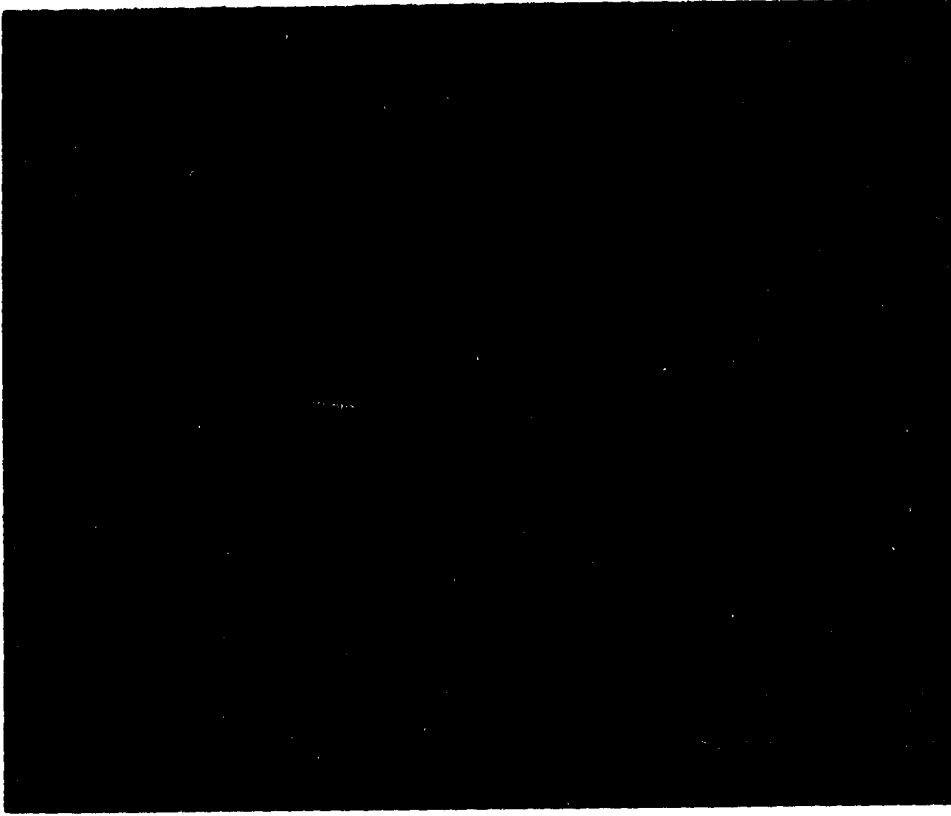


Plate 2.16
Side view, $t = 65$ ms.

The horizontal arrows indicate the position of the free surface.

5 mm

Chapter 3. Conclusions and Suggestions for Further Work

3.1. Conclusions

A sophisticated, automated apparatus has been constructed with which highly controlled impacting drop experiments can be undertaken under clean conditions. The apparatus has been constructed to allow high quality photographs to be acquired for study.

A model has been constructed of the three-dimensional vortex structure created by an impacting water drop for a very specific We and Fr . The model consists of five closed line vortices which are assembled to form a vortex skeleton. A primary vortex ring is created by the drop impact which becomes unstable. A secondary structure forms on the primary vortex ring's core and is shed into its wake in the form of three to five petals.

The generation of vorticity with opposite impulse to that of the primary ring has been observed. It is produced in the reverse impact crater and remains near the free surface. It eventually forms two concentric base rings. The appearance of the base rings is common to all the experiments undertaken including those with larger drops from a shorter fall height.

It has been observed that the shed petals are located at equal azimuthal intervals about the central axis. The petals are definitely composed of vortical fluid. This is verified by observations of the tips of the petals reconnecting to form small vortex rings which then travel away from the vortex ring's axis of symmetry. The petals' equiangular positioning is required to ensure the conservation of radially directed hydrodynamic impulse. The positions of the petals also correspond to the positions of the base

structure's spokes. At the free surface, the spokes terminate at the inner base ring. This corresponds to the vertices of the perturbed base ring.

The topology created by the drop formed vortex ring exhibits a similar three-dimensional structure to the separation bubble over a blunt flat plate. The similarity to the above-ground atomic blast is also apparent and is under investigation.

3.2. Suggestions for further work

Much work remains to fully understand this phenomena.

The very earliest stages of impact ($t < 1$ ms) is an area where much could be learned. Attempts could be undertaken to photograph the air bubble as it forms. The process of air bubble formation is an investigation which could readily be undertaken with the present apparatus. It would be valuable to obtain these photographs to understand where the sheet of trapped air is first penetrated by the impinging drop. Although the location of the bubble observed in these experiments suggests the drop liquid makes first contact at latitudes away from the central pole of the drop there are no photographs in existence which show the sheet contraction. It would be interesting to see if capillary waves on the air sheet numerically predicted by Oguz and Prosperetti (1990) for a similar configuration exist. They calculated that if a trapped axisymmetric air sheet made first contact at the centre, radially expanding capillary waves would be present that would pinch off to form unstable, toroidal bubbles. In the present case if first contact is made at regions removed from the central axis waves may appear that travel towards the central pole.

The most obvious suggestion for further work is to attempt to produce the same structure using different sized drops at the same We . This may be very difficult to

accomplish due to the drop formed structures' dependence on drop oscillation phase at impact. It remains to be seen if a similar We , Fr , Re and oscillation phase can be reproduced with other size drops.

Very fine laser sheets could be used to take sectional views of the structure during its evolution. This type of flow visualization may reveal the origin of the azimuthal phase lock observed within the structure.

Further work remains in order to understand the effect of temperature on the experiment. Variations of $3\text{ }^{\circ}\text{C}$ show a marked change in the phenomenon in preliminary experiments. It is suspected that the alteration of the structure is a result of the variation in viscosity and surface tension and the resulting change in Re and We .

The effect of the drop's oscillation phase as it impacts requires further investigation. It is known that the geometry of the free surface is significantly altered depending on the drop's phase at impact. The previous work undertaken by Rodriguez and Mesler (1988) was only for the most extreme case and much remains to be learned about the vortex-free-surface production and interaction during impact. This is expected to cause a change in the amount and initial distribution of vorticity generated due to the altered curvature at the free surface. This may lead to a technique where the initial distribution of vorticity could be altered in a controlled manner.

Work could be undertaken to estimate the amount of vorticity generated. This may be done by tracking the free surface curvature with time and estimating the vorticity required to satisfy the kinematic constraints. This would also require a method to estimate the tangential velocity q . Since much of the vorticity at the free surface separates from it to form a vortex ring the estimated amount of vorticity produced could be checked with vortex ring circulation calculations (see appendix 3). Knowledge of the amount of vorticity produced through the vortex ring calculation could also lead to

criteria for introducing vortical fluid into the irrotational flow in many of the present day boundary integral numerical methods (see for instance Baker, Meiron and Orszag 1982). These methods utilize a vortex sheet of varying strength to simulate the free surface in an otherwise wholly irrotational flow.

References for Chapter 3

- Baker G.R. Meiron D.I. and Orszag S.A. 1982 Generalized vortex methods for free surface flow problems. *J.Fluid Mech.* **123**, 477-501.
- Oguz H.N. and Prosperetti A. 1990 Bubble entrainment by the impact of drops on a liquid surface, *J. Fluid Mech.*, **219**, 143-179
- Rodriguez F. and Mesler R. 1988 The penetration of drop-formed vortex rings into pools of liquid. *J. Colloid Interface Sci.* **121**, 121-129.

Appendix 1. Automation of the apparatus and computer program listing

A computer program was written which would operate the input and output devices used in this experiment. The code was written using Quick-Basic and was run on an IBM PC. The number of drops produced in an experimental run was only limited by the amount of film on a roll. Usually 24 exposure rolls of Ektachrome 400 ASA film were used. This also limited the amount of background dye contamination in the photographs.

Once begun, the computer program operated the experiment in every respect. A description of a typical experimental run follows.

First, the operator inputs the requisite data for each drop to be formed in the course of an experimental run. This consists of: inputting the number of exposures, the rate at which the stepper motor is to be run to form the pendant drop, the rate at which the stepper motor is run to release the drop, the height from which the drops are released, the delay time for the strobe to be discharged after the laser is interrupted for each experiment, and the time to lie dormant between drops.

If it is assumed that the apparatus is initially dormant, the experiment proceeds as follows. First, the stepper motor is run at the preset forming rate. When the pendant drop reaches 90 % of a preset predicted volume the program initiates a subroutine which runs the stepper motor at the slower releasing rate. At the same time the photo-transistor circuit, which receives the laser beam is activated, the room lights are extinguished and the camera shutter is opened. The experiment is in this configuration until the pendant drop falls away from the tip. This typically requires 30 to 60 seconds.

The drop separates from the tip. The laser beam is interrupted by the impacting drop and a timer is started. The timing is performed with an external 1 MHz oscillator.

This gives a $1\ \mu\text{s}$ resolution. At the specified delay value a pulse is sent to a General Radio type 1540 Strobolume control box from the DA/M (Data Acquisition/Management board Model 000-100, manufactured by the DA/M Corporation, Edmonton, Alberta). The stock Strobolume control-box was modified in the stage 3 apparatus to eliminate a $300\ \mu\text{s}$ inherent electronic delay. This has reduced the electronic delay to a value not measurable. The flash duration for the lamp intensity used here is specified as $15\ \mu\text{s}$. After the drop interrupts the laser beam a message is sent to halt the stepper motor. The number of steps required to produce each drop is stored in an array.

A message is issued by the computer after the set delay time to close the camera shutter and turn the room lights on. The cell temperature and room temperature are recorded and stored in two arrays. The temperatures are recorded using an Analog Devices 590 solid state temperature transducer which was calibrated against a mercury thermometer.

The experiment lies dormant until the set delay between drops expires. This is measured using the computer's internal clock.

Once the program finishes the required number of experiments the data are stored on a disk. At this time the drop diameter is calculated from the number of steps required to produce a drop. Using the stored cell temperature data, the viscosity and surface tension were calculated. The impact velocity was calculated using the drop height minus one calculated drop diameter. With these values each drop's We and Fr were calculated and stored. Using this apparatus it is possible to look back at each drop experiment and determine its characteristics.

For future work it is suggested that a surface tension measurement device be constructed to give a measured value for the surface tension with time. This data would then be stored in the computer and used for the calculations of the dimensionless

numbers. Also it is suggested that the height of the hypodermic be automated via a stepper-motor controlled traverse to allow a variable height throughout an experimental run. The experiment may then automatically compensate for fluctuations in drop size (and perhaps surface tension) by creating an algorithm which alters the drop height based on the size of the previously produced drops and current fluid properties.

The following is a listing of the computer code used to operate the experiment named NEWDROP.

```

DECLARE SUB CURSLOC (cursrow!, curscol!)
DECLARE SUB CURSPLACE (rows!, cols!)
DECLARE SUB STORE ()
DECLARE SUB KEYBUF ()
DECLARE SUB TRANSEXPOS ()
DECLARE SUB SHOWEXPOS ()
DECLARE SUB EXPOSURES ()
DECLARE SUB TRANSLATE ()
DECLARE SUB EDITOR (text$, leftcol!, rightcol!, KEYCODE!, forcolor!, bakcolor!)
DECLARE SUB USERDAT ()
DECLARE SUB HILITE (fore!, back!, WINDNUM!)
DECLARE SUB NOKEYSON ()
DECLARE SUB NOKEYSOFF ()
DECLARE SUB MOTORSTEP2 (dway%, pulses!, speed!)
DECLARE SUB PORTB (BIT!)
DECLARE SUB PORTALOW (BIT!)
DECLARE SUB PORTA (BIT!)
DECLARE SUB VALIDATE (request$)
DECLARE SUB DELAY ()
DECLARE SUB CLMESS ()
DECLARE SUB KEYSET ()
DECLARE SUB MOTORSTEP (direct%, numpulse, rate)
DIM L$(50), row(50), colends(50, 4)
DIM stcol(50), nfore(50), nback(50), hifore(50), hiback(50), num$(50)
COMMON SHARED L$, row(), stcol(), numlabel, nfore(), nback(), hifore(), hiback()
COMMON SHARED colends(), scr1ptr, num$()
COMMON SHARED b$, count, basadr, direct%, rate, numpulse, timeoutval, erflag
COMMON SHARED height, sumstep, curframe, dvals(), framenum, rrates, numpulse,
timebtwx
COMMON SHARED form1$, name$, crow, ccol, temp1(), temp2(), rh()

```

```
DIM temp1(50), temp2(50), rh(50)
form1$ = "## ####.###" 'FORMAT OF FRAME AND DELAYTIME
basadr = &H300 'This is the base address for your pio96 board
```

```
'(i.e. where it is located in the computers i/o space)
```

```
OUT basadr + 3, &H82
```

```
'This command sends the value hexadecimal 82 to the location
'on the board (300 hex + 3) that is the control register.
'this register is responsible for the configuration of the
'group of ports (located on connector J1) The value hex 82 will
'configure the ports as follows: port A and C for output
'and port B for inputs.
'This completes the initialization process.
```

```
CLS
```

```
CALL KEYBUF 'Clears the keyboard buffer
```

```
CALL KEYSET 'Sets up the function key names
```

```
'The following specifies which subroutine is called by each key
```

```
ON KEY(1) GOSUB INITIALIZE
ON KEY(2) GOSUB SETUP
ON KEY(3) GOSUB START
ON KEY(4) GOSUB HALT
ON KEY(6) GOSUB PRNT
ON KEY(7) GOSUB FINI
ON KEY(8) GOSUB NOISE
ON KEY(9) GOSUB REWIN
ON KEY(10) GOSUB DISK
```

```
.....
```

```
'Activate keys.
```

```
KEY(1) ON
```

```
KEY(2) ON
```

```
KEY(3) ON
```

```
KEY(4) ON
```

```
KEY(6) ON
```

```
KEY(7) ON
```

```
KEY(8) ON
```

```
KEY(9) ON
```

```
KEY(10) ON
```

```
.....
```

```

CLOSE
REM -- Runs 2400 baud to the DA/M through the special communication cable.

'Set serial port 1 to 2400 baud, no parity, 8 data, one stop, ignore carrier detect
'data set ready, and request to send lines.

OPEN "com1:2400,n,8,1,CD0,DS0,RS" FOR RANDOM AS #1

ON COM(1) GOSUB 400 'Serial communication routine at label 400

COM(1) ON

REM -- You must have pin 20 (DTR) wired to pin 6 (DSR) and
REM -- Also pin 4 (CTS) wired to pin 5 (RTS) for this software to work.

    LOCATE 1, 1
    PRINT "DA/M Communications"
    COL = 1
    framenum = 24 'Default number of frames see also the value of num$(6) below.

    L$(1) = "TEST NAME " 'Text for the labels on the screen.
    L$(2) = "FORMING PULSES "
    L$(3) = "FORMING RATE "
    L$(4) = "RELEASE PULSES "
    L$(5) = "RELEASE RATE "
    L$(6) = "EXPOSURES "
    L$(7) = "TIMEOUT VALUE "
    L$(8) = "TIME BETWEEN EXPOSURES "
    L$(9) = "DROP HEIGHT "

    FOR i = 10 TO 45
        L$(i) = "" 'Text for the labels of frame and delay listing (no labels).
    NEXT

    stcol(1) = 1 'Starting column for text labels above.
    stcol(2) = 1
    stcol(3) = 1
    stcol(4) = 25
    stcol(5) = 25
    stcol(6) = 50
    stcol(7) = 50
    stcol(8) = 25
    stcol(9) = 51

```

```

FOR i = 10 TO 21
    stcol(i) = 1 'No labels for frame and delay listing
NEXT

FOR i = 22 TO 34
    stcol(i) = 25 'Frame and delay listing is in 3 columns this is 2.
NEXT

FOR i = 35 TO 47
    stcol(i) = 50 'This is 3.
NEXT

num$(1) = " "
num$(2) = "1500"
num$(3) = "1" 'Default values for the corresponding labels
num$(4) = "2000" 'ie. num$(1) for L$(1).
num$(5) = "10"
num$(6) = "20"
num$(7) = "500"
num$(8) = "3"
num$(9) = "35.5"

FOR i = 10 TO 47 'No labels for frame and delay so no defaults.
    num$(i) = ""
NEXT

numlabel = 9 'Max number of labels to show

FOR i = 1 TO 47
    nfore(i) = 7 'Fore ground and background colors
    nback(i) = 0
    hifore(i) = 0 'Hilited foreground and background
    hiback(i) = 7
NEXT

colends(1, 1) = 11
colends(2, 1) = 16
colends(3, 1) = 14
colends(4, 1) = 40 'starting columns for editing fields are
colends(5, 1) = 38 'in dimension colends(x,1)
colends(6, 1) = 60
colends(7, 1) = 64
colends(8, 1) = 48
colends(9, 1) = 63

```

```

FOR i = 10 TO 21
    colends(i, 1) = 5
    colends(i, 2) = 13    'Ending columns for editing field are in
    row(i) = i - 6        'colends(x,2)
NEXT

```

```

FOR i = 22 TO 33
    colends(i, 1) = 30
    colends(i, 2) = 38
    row(i) = i - 18
NEXT

```

```

FOR i = 34 TO 45
    colends(i, 1) = 55
    colends(i, 2) = 63
    row(i) = i - 30
NEXT

```

```

colends(1, 2) = colends(1, 1) + LEN(num$(1)) 'Ending columns for editing field are
colends(2, 2) = colends(2, 1) + LEN(num$(2)) 'colends(x,2)
colends(3, 2) = colends(3, 1) + LEN(num$(3))
colends(4, 2) = colends(4, 1) + LEN(num$(4))
colends(5, 2) = colends(5, 1) + LEN(num$(5))
colends(6, 2) = colends(6, 1) + LEN(num$(6))
colends(7, 2) = colends(7, 1) + LEN(num$(7))
colends(8, 2) = colends(8, 1) + LEN(num$(8))
colends(9, 2) = colends(9, 1) + LEN(num$(9))

```

```

row(1) = 19
row(2) = 20
row(3) = 21 'Rows for the editing fields.
row(4) = 20
row(5) = 21
row(6) = 20
row(7) = 21
row(8) = 22
row(9) = 22

```

```

FOR i = 1 TO framenum + 10
    COLOR nfore(i), nback(i) 'Print the delay times and frame number on screen.
    LOCATE row(i), stcol(i)
    PRINT L$(i); num$(i);
NEXT

```

```

'-----
LOCATE 1, 22, 0 'Place in damcom area and shutoff cursor blink.
CALL CURSLOC(crow, ccol)

WHILE 1

WEND      'Infinite loop. Program hangs here until called to a subroutine
          'by the function keys.
END       'End of program

.....

***** SUBROUTINES *****

INITIALIZE:

MASTERSET:  CMD$ = "T0,4H2001F807"
            CALL VALIDATE(CMD$) 'Sends cmd$ to the dam board

QUADOFF:    CMD$ = "T1,1HC0"
            CALL VALIDATE(CMD$)

ICRSET:     CMD$ = "T1,1H58"
            CALL VALIDATE(CMD$)

OCRSET:     CMD$ = "T1,1H92"
            CALL VALIDATE(CMD$)
            PRINT #1, "D1"
            CALL CLMESS 'clears the message area and locates the cursor
            PRINT "INITIALIZATION COMPLETE"

CALL CURSPLACE(crow, ccol)

RETURN

400 'Serial communication subroutine (dam board)
COM(1) OFF 'Shut off the com trap (so this routine doesn't get called now)
CALL NOKEYSON 'Shut off the function keys
COLOR 0, 7
WHILE NOT EOF(1) 'Ensure the end of the communication buffer has not been
reached.

```

```

a$ = INPUT$(1, #1) 'Input 1 char. from com buffer.
IF a$ = CHR$(13) OR a$ = CHR$(10) THEN a$ = " "

IF a$ = ">" THEN
    PRINT ">";
    FOR i = 1 TO 500
    NEXT
    LOCATE 1, 22
    PRINT SPACES$(57); 'If it is, clear the DA/M com screen area
    LOCATE 1, 22
    b$ = b$ + a$      'Store the complete message in b$.
ELSE
    PRINT a$; 'Print the char. in the dam com screen area
    b$ = b$ + a$ 'Append the char. onto b$
END IF
WEND

```

```

CALL NOKEYSOFF 'turn the function keys back on
COM(1) ON 'turn the com trapback on
COLOR 7, 0

```

RETURN

SETUP:

```

CALL KEYBUF 'Clear the keyboard buffer

scr1ptr = 1 'Default label to set the cursor on
CALL HILITE(hifore(scr1ptr), hiback(scr1ptr), scr1ptr) 'Hilite the area
                                                    'where data is entered.

CALL KEYBUF 'Clear the keyboard buffer.
CALL CLMESS
PRINT "(esc key to edit delay times)"
CALL CURSPLACE(crow, ccol)
CALL USERDAT 'Routine to enter data
CALL CLMESS
CALL TRANSLATE 'Translate the entered data (characters) into numerics
CALL CURSPLACE(crow, ccol)
CALL SHOWEXPOS 'Print out the frame/delay table
CALL CURSPLACE(crow, ccol)
CALL KEYBUF
CALL CLMESS

```



```

PRINT "(esc key to exit edit mode)"
CALL CURSPLACE(crow, ccol)
CALL EXPOSURES 'Routine to edit the frame delay table
CALL CURSPLACE(crow, ccol)
CALL TRANSEXPOS 'Translate the edited table(char.) into numerics
CALL CURSPLACE(crow, ccol)
CALL SHOWEXPOS 'Print out table
CALL CLMESS
CALL CURSPLACE(crow, ccol)

LOCATE 1, 1
PRINT "DA/M Communications"
CALL CURSPLACE(crow, ccol)
RETURN

START:
CALL TRANSLATE 'Be sure both data fields have been translated
CALL TRANSEXPOS 'to ensure that if the user depresses start without exiting
                  'the edit functions

FOR w = 1 TO framenum
    dvals(w, 3) = 0
NEXT

FOR curframe = 1 TO framenum 'Main loop for individual drop production
                              sequence.

    IF NOISEFLAG THEN          Siren loop "optional"

        FOR p = 100 TO 500 STEP 5
            SOUND p, 1
        NEXT

        SOUND 500, 5
        FOR p = 500 TO 100 STEP -5
            SOUND p, 1
        NEXT

    END IF

REPEAT:    LOCATE 22, 1
          PRINT "CURRENT FRAME IS "; curframe

```

```

CALL CURSPLACE(crow, ccol)
CALL PORTA(&H4)      'Send Porta the position of the bit ie 4=BIT
                      position 3
                      'Take it high
CALL PORTALOW(&H4)   'Take it low
STATE = 2
CALL PORTB(STATE)    'Read BIT POSITION 2 (SECOND BIT) return
                      'The value in state (2=on 0=off)
IF STATE THEN        'If state is not 0 (ie 2)
  CALL CLMESS

  PRINT "INPUT NOT RESET, CHECK SYSTEM, ANY KEY TO
RESUME"

  CALL CURSPLACE(crow, ccol)
  DUMP$ = ""          'Wait for the key press and when you get it,

  WHILE DUMP$ = ""    'delete it.
    DUMP$ = INKEY$
  WEND

  GOTO REPEAT        'Have received the key press now, try the frame
                      again

END IF

h$ = HEX$(dvals(curframe, 1) * 1000) 'Convert the delay value for
WHILE LEN(h$) < 6          'this frame to 6 digit hex
  h$ = "0" + h$
WEND

CMD$ = "T1,4HD8" + h$      'and send the load preset reg.
CALL VALIDATE(CMD$)        'command to the DA/M.
CMD$ = "T1,1HE8"
CALL VALIDATE(CMD$)
CALL PORTA(&H8)      'Send PORTA the position of the bit ie 8 = BIT
                      ' POSITION 4

CALL PORTALOW(&H8)    'take it high then low
STATE = 1
CALL PORTB(STATE)    'BIT POSITION 0 (first BIT)

IF STATE THEN        'read the state of the first bit on PORTB
  CALL CLMESS

```

```

PRINT "OUTPUT NOT RESET, ANY KEY TO RESUME"
CALL CURSPLACE(crow, ccol)
DUMP$ = ""

```

```

WHILE DUMP$ = ""
DUMP$ = INKEY$
WEND

```

```

GOTO REPEAT
END IF

```

```

CALL MOTORSTEP(0, numpulse, rate) 'Initiate the production of the
                                   drop production sequence. This
                                   sequence fills the drop up to 90% of
                                   the predicted final volume.

```

```

PRINT #1, "D0"

```

```

FOR i = 1 TO 100 'Artificial delay
NEXT i

```

```

CALL PORTA(&H10) 'Send PORTA the position of the bit ie.
16=BIT POSITION 5
' This will open the camera shutter

```

```

CALL MOTORSTEP2(0, numpulse, rrate) 'This produces steps to fill the
                                      pendant drop to the point where it
                                      will release from the hypodermic
                                      tube.

```

```

CALL PORTALOW(&H10) 'Close the camera's shutter.

```

```

CALL DELAY

```

```

PRINT #1, "D1" 'digital output

```

```

FOR i = 1 TO 500 'Artificial delay imposed on program to ensure DA/M
                  communications operate smoothly.
NEXT i

```

```

b$ = ""

```

```

PRINT #1, "A1" 'Analog input chan 1, temperature from the test cell.

```

```

FOR i = 1 TO 500

```

```

NEXT i          'Artificial delay imposed on program to ensure
                DA/M communications operate smoothly.

```

```

b$ = MID$(b$, 3)
templ(curframe) = VAL(b$)

```

```

b$ = ""
PRINT #1, "A2"  'Analog input chan 2, relative humidity.

```

```

FOR i = 1 TO 500  'Artificial delay.
NEXT i

```

```

b$ = MID$(b$, 3)
rh(curframe) = VAL(b$)

```

```

b$ = ""
PRINT #1, "A3"  'Analog input chan 3, ambient temperature.

```

```

FOR i = 1 TO 500  'Artificial delay.
NEXT i

```

```

b$ = MID$(b$, 3)
temp2(curframe) = VAL(b$)

```

```

b$ = ""

```

```

CALL CLMESS
PRINT "INTER-EXPOSURAL PAUSE"

```

```

CALL CURSPLACE(crow, ccol)
SLEEP timebtwx * 60      'Delay time between exposures

```

WHILE HALTFLAG 'If the halt flag has been set (key f4 has
'been pressed), then wait here until repress.

CALL CLMESS
PRINT "PROGRAM PAUSED" 'Pause main sequence option.

WEND

CALL CURSPLACE(crow, ccol)
CALL CLMESS

NEXT curframe 'Continue with next experiment in main loop.

CALL CURSPLACE(crow, ccol)

RETURN

.....

HALT: 'Halt/resume toggle routine

HALTFLAG = NOT HALTFLAG

IF HALTFLAG THEN

KEY 4, "RESUME"
CALL CLMESS
PRINT "PROGRAM WILL PAUSE AFTER COMPLETION OF THIS

FRAME"

ELSE

KEY 4, "PAUSE"
CALL CLMESS

END IF

CALL CURSPLACE(crow, ccol)

RETURN

PRNT: 'Print out to printer routine

LPRINT name\$

LPRINT "STEPS TO FORM DROP: "; TAB(40); numpulse

```

LPRINT "PULSE RATE TO FORM DROP: "; TAB(40); rate
LPRINT "MAX STEPS TO RELEASE DROP: "; TAB(40); mumpulse
LPRINT "RELEASE PULSE RATE: "; TAB(40); rrate
LPRINT "TIMEOUT VALUE (s): "; TAB(40); timeoutval
LPRINT "TIME BETWEEN EXPOSURES (MIN): "; TAB(40); timebtwx
LPRINT
LPRINT
LPRINT "FRAME    DELAY (ms)"
FOR i = 1 TO framenum
'print out the frame number and the delay and an X if a flag
'has been set in the array dvals(x,2) note: flag should be
'set to a -1 or a 1 to print an X.
'temp1(i) = temp1(i) / 255 * 15 + 15
'temp1(i) = temp1(i) * 10
'temp1(i) = INT(temp1(i))
'temp1(i) = temp1(i) / 10
'temp2(i) = temp2(i) / 255 * 15 + 15
'temp2(i) = temp2(i) * 10
'temp2(i) = INT(temp2(i))
'temp2(i) = temp2(i) / 10
'rh(i) = rh(i) / 255 * 91.8
'rh(i) = rh(i) * 10
'rh(i) = INT(rh(i))
'rh(i) = rh(i) / 10
LPRINT i; " "; TAB(5); dvals(i, 1); TAB(14); "ms";
LPRINT CHR$(ABS(dvals(i, 2)) * 88);
LPRINT TAB(20); dvals(i, 3); TAB(25); " steps";
LPRINT TAB(32); "cell "; temp1(i); " deg C";
LPRINT TAB(48); rh(i); "%"; TAB(54); "amb ";
LPRINT temp2(i); " deg C"
NEXT i

```

RETURN

DISK:

CALL STORE 'store the data on disk in the same form as the print out
RETURN

FINI: ' make sure file saved and end program
CLS

```

LOCATE 10, 20
PRINT "file saved? y/n"
'jackdaws love my big sphinx of quartz
WHILE q$ = ""
  q$ = INKEY$
WEND
IF q$ = "n" OR q$ = "N" THEN
  CALL STORE
ELSE END
END IF
q$ = ""
RETURN

```

```

'.....:
,

```

NOISE: 'Allows siren to be turned on which warns operator of approaching experiment.

```

NOISEFLAG = NOT NOISEFLAG
IF NOISEFLAG THEN
  KEY 8, "SOUND"
ELSE
  KEY 8, "QUIET"
END IF
CALL CURSPLACE(crow, ccol)
RETURN

```

```

'.....:

```

REWIND: Allows operator to rewind piston after an experimental run. The operator can rewind the piston to the original starting location or any number of steps specified by the operator.

CALL CLMESS 'Clears message area

```
r$ = ""
```

```
PRINT "Total steps :"; sumstep; " Use this value ? Y/N"
```

```

WHILE r$ = ""
  r$ = INKEY$
WEND

```

IF r\$ = "n" OR r\$ = "N" THEN 'If user enters n, the program requires

'an arbitrary number of steps entered.

```
*****
' Remember that to retract the piston 1mm requires 6102 steps
' 155000 for 1 inch
```

```
*****
```

```
CALL CLMESS 'Clear display screen
INPUT " Number of steps = ? : ", sumstep 'Gives user the option of
                                         'using summed value of steps from
                                         'program or an arbitrary number.
```

```
END IF
```

```
CALL CLMESS 'Clear display screen
CALL MOTORSTEP(1, sumstep, 1) ' The first variable passed is direction
                               ' the second the number of steps
                               ' the third is fastest motor rate
```

```
CALL CLMESS ' Clear display screen
```

```
r$ = "" 'Set r$ back to null
```

```
RETURN
```

```
'.....
```

Errorproc: ' Detects filenames not acceptable to DOS.

```
SELECT CASE ERR
```

```
CASE 64:          'Bad file name
PRINT "**** Error bad file name****"
PRINT " Change file name, enter C; or else filter filename enter F"
'Cases available: C, F; any other gives file the name BUFFER"
```

```
a$ = ""
    WHILE a$ = ""
a$ = INKEY$
```

```
WEND
```



```

IF a$ = "c" OR a$ = "C" THEN

CLS

LINE INPUT "New file name:"; cow$
name$ = cow$

ELSEIF a$ = "F" OR a$ = "f" THEN

                                filterstring$ =
"abcdefghijklmnopqrstuvwxyz1234567890ABCDEFGHIJKLMNOPQRSTUVWXYZ"
                                'Previous line are the characters available for file name
                                'hog$ = "" dummy string which is used to build filtered file
                                'name

                                txtlength = LEN(name$)'length of original file name

                                FOR i = 1 TO txtlength ' loop to create filtered

                                    c$ = MID$(name$, i, 1) ' filename

                                    IF INSTR(filterstring$, c$) < > 0 THEN
                                        hog$ = hog$ + c$ ' add filtered
                                                                'variable to hog$
                                    END IF

                                NEXT i

                                name$ = hog$

ELSE
name$ = "buffer" 'Last resort name if f or c isn't pressed

END IF

CASE 61:
PRINT " B:\ drive full"

CASE 71:
PRINT " B:\ drive door open "

CASE 72:
PRINT " You got yourself into this one"

```

```

        END SELECT
RESUME
REM $STATIC

```

```

SUB CLMESS
COLOR 7, 0
LOCATE 23, 1
PRINT SPACE$(70)
LOCATE 23, 1, 0
END SUB

```

```

SUB CURSLOC (cursrow, curscol)
    cursrow = CSRLIN
    curscol = POS(0)

```

```

END SUB

```

```

SUB CURSPLACE (rows, cols)
LOCATE rows, cols, 0
END SUB

```

```

SUB DELAY
FOR i = 1 TO 100
NEXT
END SUB

```

```

SUB EDITOR (text$, leftcol, rightcol, KEYCODE, forcolor, bakcolor)
'don't touch this routine, it is unlikely that your problem is here.

```

```

DEF SEG = 0
IF PEEK(&H463) = &HB4 THEN
    csrsize = 12
ELSE csrsize = 7
END IF
EDIT$ = SPACE$(rightcol - leftcol + 1)
LSET EDIT$ = text$
TXTPOS = POS(0) - leftcol + 1
IF TXTPOS < 1 THEN TXTPOS = 1
IF TXTPOS > LEN(EDIT$) THEN TXTPOS = LEN(EDIT$)
LOCATE , leftcol
COLOR forcolor, bakcolor
PRINT EDIT$;

```

```

DO
LOCATE , leftcol + TXTPOS - 1, 1
  DEF SEG = &H40
  DO
    C$ROW = CSRLIN
    CURCOL = POS(0)
    KY$ = INKEY$
    LOOP UNTIL LEN(KY$) OR ((PEEK(&H17) AND &H8) = 8)
    IF LEN(KY$) = 1 THEN
      KEYCODE = ASC(KY$)
    END IF
    IF LEN(KY$) = 0 THEN
      KEYCODE = -56
    END IF
    IF LEN(KY$) = 2 THEN
      KEYCODE = -ASC(RIGHT$(KY$, 1))
    END IF
  END IF
  DEF SEG

SELECT CASE KEYCODE
CASE 8 'backspace
  TXTPOS = TXTPOS - 1
  LOCATE , leftcol + TXTPOS - 1, 0
  IF TXTPOS > 0 THEN
    IF insert THEN
      MID$(EDIT$, TXTPOS) = MID$(EDIT$, TXTPOS + 1) + " "
    ELSE
      MID$(EDIT$, TXTPOS) = " "
    END IF
    COLOR forcolor, bakcolor
    PRINT MID$(EDIT$, TXTPOS);
  END IF

CASE 13, 27, -80, -72 'enter or/ escape or/ down arrow/ or up arrow
EXIT DO
CASE 32 TO 254 'letter keys
  LOCATE , , 0 'cursor off
  IF insert THEN
    MID$(EDIT$, TXTPOS) = KY$ + MID$(EDIT$, TXTPOS)
    COLOR forcolor, bakcolor
    PRINT MID$(EDIT$, TXTPOS);

```

```

ELSE
    MID$(EDIT$, TXTPOS) = KY$
    COLOR forcolor, bakcolor
    PRINT KY$;
    END IF
    TXTPOS = TXTPOS + 1
CASE -75      'left arrow
    TXTPOS = TXTPOS - 1
CASE -77      'right arrow
    TXTPOS = TXTPOS + 1
CASE -71      'home
    TXTPOS = 1
CASE -79      'end
    FOR n = LEN(EDIT$) TO 1 STEP -1
        IF MID$(EDIT$, n, 1) < > " " THEN EXIT FOR
    NEXT
    TXTPOS = n + 1
    IF TXTPOS > LEN(EDIT$) THEN TXTPOS = LEN(EDIT$)
CASE -82      'insert key
    insert = NOT insert
    IF insert THEN
        LOCATE , , , csrsize \ 2, csrsize
    ELSE
        LOCATE , , , csrsize - 1, csrsize
    END IF
CASE -83      'delete key
    MID$(EDIT$, TXTPOS) = MID$(EDIT$, TXTPOS + 1) + " "
    LOCATE , , 0
    COLOR forcolor, bakcolor
    PRINT MID$(EDIT$, TXTPOS);
CASE -56      ' the alt key
    EXIT DO
CASE ELSE
    EXIT DO
END SELECT
IF TXTPOS > LEN(EDIT$) THEN TXTPOS = LEN(EDIT$)
IF TXTPOS < 1 THEN TXTPOS = 1
LOOP
text$ = (EDIT$)

END SUB

SUB EXPOSURES

```

```

REDIM dvals(36, 5)
scr1ptr = 10 'set the cursor to label 9
LOCATE row(scr1ptr), colends(scr1ptr, 1)
CALL EDITOR(num$(scr1ptr), colends(scr1ptr, 1), colends(scr1ptr, 2), KEYCODE,
hifore(scr1ptr), hiback(scr1ptr))
'Syntax for editor is,...
'call editor (a$,b,c,d,e,f)
'the editor will allow editing in the field described as follows
'a$=default label
'b=starting column for edit field
'c=end column for edit field
'd=.

DO
    SELECT CASE KEYCODE
        CASE 27 'esc
            EXIT DO
        CASE 13 'cr
            ' Anything else, just move down 1 item
            CALL HILITE(nfore(scr1ptr), nback(scr1ptr), scr1ptr)
            scr1ptr = scr1ptr + 1
            IF scr1ptr > framenum + 9 THEN scr1ptr = 10
            CALL HILITE(hifore(scr1ptr), hiback(scr1ptr), scr1ptr)

            LOCATE , colends(scr1ptr, 1)
            CALL EDITOR(num$(scr1ptr), colends(scr1ptr, 1),
colends(scr1ptr, 2), KEYCODE, hifore(scr1ptr), hiback(scr1ptr))

            'cursor control
        CASE -80 'move down
            CALL HILITE(nfore(scr1ptr), nback(scr1ptr), scr1ptr)
            scr1ptr = scr1ptr + 1
            IF scr1ptr > framenum + 9 THEN scr1ptr = 10
            CALL HILITE(hifore(scr1ptr), hiback(scr1ptr), scr1ptr)
            LOCATE , colends(scr1ptr, 1)
            CALL EDITOR(num$(scr1ptr), colends(scr1ptr, 1),
colends(scr1ptr, 2), KEYCODE, hifore(scr1ptr), hiback(scr1ptr))
        CASE -72 'Move up
            CALL HILITE(nfore(scr1ptr), nback(scr1ptr), scr1ptr)
            scr1ptr = scr1ptr - 1
            IF scr1ptr < 10 THEN scr1ptr = framenum + 9
            CALL HILITE(hifore(scr1ptr), hiback(scr1ptr), scr1ptr)
            LOCATE , colends(scr1ptr, 1)

```

```

CALL EDITOR(ram$(scr1ptr), colends(scr1ptr, 1),
colends(scr1ptr, 2), KEYCODE, hifore(scr1ptr), hiback(scr1ptr))
CASE -77 'Move left
LOCATE , colends(scr1ptr, 1)
CALL EDITOR(num$(scr1ptr), colends(scr1ptr, 1),
colends(scr1ptr, 2), KEYCODE, hifore(scr1ptr), hiback(scr1ptr))
CASE -75 'Move right

LOCATE , colends(scr1ptr, 1)
CALL EDITOR(num$(scr1ptr), colends(scr1ptr, 1),
colends(scr1ptr, 2), KEYCODE, hifore(scr1ptr), hiback(scr1ptr))
CASE -56 'ALT
LOCATE , colends(scr1ptr, 1)
CALL EDITOR(num$(scr1ptr), colends(scr1ptr, 1),
colends(scr1ptr, 2), KEYCODE, hifore(scr1ptr), hiback(scr1ptr))
CASE ELSE
LOCATE , colends(scr1ptr, 1)
CALL EDITOR(num$(scr1ptr), colends(scr1ptr, 1),
colends(scr1ptr, 2), KEYCODE, hifore(scr1ptr), hiback(scr1ptr))
END SELECT
LOOP

```

END SUB

SUB FETCHKEY (KEYCODE)

DEF SEG = &H40

DO

KY\$ = INKEY\$

LOOP UNTIL LEN(KY\$) OR (PEEK(&H17) AND &H8) = 8

DEF SEG

IF LEN(KY\$) = 1 THEN

KEYCODE = ASC(KY\$)

END IF

IF LEN(KY\$) = 0 THEN

KEYCODE = -56

END IF

IF LEN(KY\$) = 2 THEN

KEYCODE = -ASC(RIGHT\$(KY\$, 1))

END IF

END SUB

```

SUB HILITE (fore, back, WINDNUM)
COLOR fore, back
LOCATE row(WINDNUM), stcol(WINDNUM)
PRINT L$(WINDNUM);
LOCATE , colends(WINDNUM, 1)
PRINT num$(WINDNUM);
END SUB

```

```

SUB KEYBUF
'empty keyboard buffer
DEF SEG = &H0
POKE &H41C, (PEEK(&H41A))
POKE &H41D, (PEEK(&H41B))
DEF SEG

```

```

END SUB

```

```

SUB KEYSET
KEY ON
KEY 1, "INIT"
KEY 2, "SETUP"
KEY 3, "START"
KEY 4, "PAUSE"
KEY 6, "PRINT"
KEY 7, "QUIT"
KEY 8, "QUIET"
KEY 9, "REWIND"
KEY 10, "SAVE"
END SUB

```

```

SUB MOTORSTEP (direct%, numpulse, rate)
  'SET DIRECTION
  CALL CLMESS
  IF direct% = 0 THEN PRINT "FORMING DROP"
  IF direct% = 1 THEN PRINT "REWINDING PISTON"

  OUT basadr, INP(basadr) OR direct%      'SET THE DIRECTION LINE

  ONCODE% = direct% OR 2                  'CALCULATE THE VALUES FOR
DIRECTION
  OFFCODE% = &HFD                        'WITH PULSE LINE HI AND LO

```

```

FOR i = 0 TO numpulse
  OUT basadr, INP(basadr) OR ONCODE%      'PULSE LINE HI
    FOR J = 0 TO rate      'DELAY TIME
    NEXT J
  OUT basadr, INP(basadr) AND OFFCODE%    'PULSE LINE LO
    FOR J = 0 TO rate      'DELAY TIME
    NEXT J

NEXT i

END SUB

SUB MOTORSTEP2 (dway%, pulses, speed)
  CALL CLMESS
  PRINT "RELEASING DROP"
  OUT basadr, INP(basadr) OR dway%      'SET THE DIRECTION LINE

  ONCODE% = dway% OR 2      'CALCULATE THE VALUES FOR
  DIRECTION
  OFFCODE% = &HFD      'WITH PULSE LINE HI AND LO
  TIMES$ = "00:00:00"

  DO UNTIL i > pulses OR iset OR TIMER > timeoutval
    iset = 2
    CALL PORTB(iset)      'BIT POSITION 2 (SECOND BIT)

    OUT basadr, INP(basadr) OR ONCODE%    'PULSE LINE HI
      FOR J = 0 TO speed      'DELAY TIME
      NEXT J
    OUT basadr, (INP(basadr) AND OFFCODE%) 'PULSE LINE LO
      FOR J = 0 TO speed      'DELAY TIME
      NEXT J
    dvals(curframe, 3) = i
    i = i + 1

  LOOP

  dvals(curframe, 3) = (dvals(curframe, 3) + numpulse) ' This stores the number
                                                         of total steps required to
                                                         make a drop.

  sumstep = sumstep + dvals(curframe, 3) 'Sums the total number of steps in an
                                         'in an experiment for rewinding the piston

```


'to initial position

```

IF iset THEN                                     ' Counts to time out value
    erflag = 0
    iset = 0
    TIMES$ = "00:00:00"
    DO UNTIL iset OR TIMER > timeoutval
        iset = 1
        CALL PORTB(iset)
    LOOP
    IF iset < > 1 THEN
        CALL CLMESS
        PRINT "input set but output not set, get professional help";
        CALL PORTALOW(&H10)
        CALL STORE
        STOP
    END IF

ELSE
    erflag = erflag + 1'increment errorflag
    and (frame, 2) = 1
END IF

IF erflag > 1 THEN
    CALL CLMESS
    PRINT "input line not set,check system (motorstep2)"
    CALL PORTALOW(&H10)
    CALL STORE
    STOP
END IF

END SUB

SUB KEYSOFF
KEY(1) ON
KEY(2) ON
KEY(3) ON
KEY(4) ON
KEY(6) ON
KEY(7) ON
KEY(9) ON
KEY(10) ON

END SUB

```

SUB NOKEYSON

KEY(1) OFF

KEY(2) OFF

KEY(3) OFF

KEY(4) OFF

KEY(6) OFF

KEY(7) OFF

KEY(9) OFF

KEY(10) OFF

END SUB

SUB PORTA (BIT)

CURSTATE = INP(basadr)

OUT basadr, (CURSTATE OR BIT)

END SUB

SUB PORTALOW (BIT)

BIT = BIT XOR &H255

CURSTATE = INP(basadr)

OUT basadr, (CURSTATE AND BIT)

END SUB

SUB PORTB (BIT)

CURSTATE = INP(basadr + 1)

BIT = CURSTATE AND BIT

END SUB

SUB PORTBLOW (BIT)

BIT = BIT XOR &H255

CURSTATE = INP(basadr + 1)

OUT basadr + 1, (CURSTATE AND BIT)

END SUB

SUB PORTC (BIT)

CURSTATE = INP(basadr + 2)

OUT basadr + 2, (CURSTATE OR BIT)

END SUB

```

SUB PORTCLOW (BIT)
    BIT = BIT XOR &H255
    CURSTATE = INP(basadr + 2)
    OUT basadr + 2, (CURSTATE AND BIT)
END SUB

```

```

SUB SHOWEXPOS

```

```

    COLOR 7, 0

```

```

    FOR i = 4 TO 16
        LOCATE i, 1
        PRINT SPACE$(79);
    NEXT

```

```

    COL = 1
    FOR i = 1 TO framenum
        SELECT CASE i
            CASE IS < 13
                LOCATE 3, 1
                PRINT "No. delay (ms)";
                LOCATE i + 3, COL
                PRINT USING form1$; i; dvals(i, 1);
            CASE 13 TO 24
                LOCATE 3, 26
                PRINT "No. delay (ms)"
                LOCATE i - 9, COL + 25
                PRINT USING form1$; i; dvals(i, 1);
            CASE IS > 24
                LOCATE 3, 51
                PRINT "No. delay (ms)"
                LOCATE i - 21, COL + 50
                PRINT USING form1$; i; dvals(i, 1);
            CASE ELSE
        END SELECT
    NEXT
    LOCATE , , 0

```

```

END SUB

```

```

SUB STORE
    ON ERROR GOTO Errorproc

```

```

OPEN "b:" + LEFT$(name$, 8) FOR OUTPUT AS 2
PRINT #2, name$
PRINT #2, "STEPS TO FORM DROP: "; TAB(40); numpulse
PRINT #2, "PULSE RATE TO FORM DROP: "; TAB(40); rate
PRINT #2, "MAX STEPS TO RELEASE DROP: "; TAB(40); rnumpulse
PRINT #2, "RELEASE PULSE RATE: "; TAB(40); rrate
PRINT #2, "TIMEOUT VALUE (s): "; TAB(40); timeoutval
PRINT #2, "TIME BETWEEN EXPOSURES (MIN): "; TAB(40); timebtwx
PRINT #2, "RELEASE HEIGHT (mm):"; TAB(40); height
PRINT #2,
PRINT #2,
PRINT #2, " FRAME  DELAY (ms)  STEPS  CF  (C)  RH(%)  AMB (C)
dia"

```

```

'Calculate impact velocity.
height = height / 10 ' cm

```

```

FOR i = 1 TO framenum
    temp1(i) = temp1(i) / 255 * 15 + 15 'Calculates cell temperature
    temp1(i) = temp1(i) * 10
    temp1(i) = INT(temp1(i))
    temp1(i) = temp1(i) / 10

    temp2(i) = temp2(i) / 255 * 15 + 15 'Calculates ambient
temperature
    temp2(i) = temp2(i) * 10
    temp2(i) = INT(temp2(i))
    temp2(i) = temp2(i) / 10

    rh(i) = rh(i) / 256 * 91.8          ' Calculates relative humidity
    rh(i) = rh(i) * 10
    rh(i) = INT(rh(i))
    rh(i) = rh(i) / 10

    'Calculate the fluid properties

    ro = .998 ' gm/cm^3
    ,
    '.....
    mu = .001792 'kg/(m*s)
    mu = mu / 100 'kg/(cm*s)
    mu = mu * 1000 'gm/(cm*s)

```

Tho = 273.15 'deg K
 Th = temp1(i) + 273.15 'deg K

a = -1.94 ' Emperical constants for equation below
 b = -4.8
 c = 6.74

' Equation from White page 20.

visc = mu * (EXP(a + b * (Tho / Th) + c * (Tho / Th) ^ 2))

'.....
 ' Calculation for Surface Tension

Temp = temp1(i)

Calculated using a third order polynomial fit
 ' on GRAPHER

gamma = 75.68 - .138 * Temp - .000326702# * Temp ^ 2 +
 .000000361804# * Temp ^ 3' dynes/cm

'.....

'Find length of piston stroke

stroke = dvals(i, 3) / 6102 'mm

'piston diameter 1/4 inch, convert to mm from inches

dia = .25 * 25.04

' Calculate drop radius

dd = ((1.5 * stroke) ^ (.33333)) * ((dia) ^ (.66667))

' Convert to cm from mm

dd = dd / 10 'cm

fallh = height - dd 'modify to account for drop diameter

U = (2 * 981 * fallh) ^ (.5) ' cm/s 'impact velocity

'Calculate Froude number

IF ABS(dd) > 0 THEN Fr = (U ^ 2) / (981 * dd)

```

'Calculate Weber number

IF ABS(gamma) > 0 THEN We = (ro * (U ^ 2) * dd) / gamma

'Calculate Reynolds number of the falling drop.

IF ABS(visc) > 0 THEN Re = ro * U * dd / visc

PRINT #2, i; " "; TAB(9); dvals(i, 1);
      PRINT #2, CHR$(ABS(dvals(i, 2)) * 88);
      PRINT #2, TAB(23); dvals(i, 3);
      PRINT #2, TAB(30); temp1(i); "C"; TAB(41); rh(i); "%";
      PRINT #2, TAB(49); temp2(i); "C";
      PRINT #2, TAB(1); "drop dia="; dd; " Fr="; Fr; " We="
"; We; " Re="; Re;
      PRINT #2, " Nu ="; visc; "Gamma"; gamma; "U="; U
NEXT i

CLOSE 2
END SUB

```

SUB TRANSEXPOS

FOR i = 1 TO framenum

dvals(i, 1) = VAL(num\$(i + 9))

IF dvals(i, 1) / 1000 >= timeoutval THEN

dvals(i, 1) timeoutval * 1000

END IF

IF dvals(i, 1) > 17777 THEN dvals(i, 1) = 17777 'Maximum delay = 17.7
seconds

NEXT

END SUB

SUB TRANSLATE

rate = VAL(num\$(3))

numpulse = VAL(num\$(2))

rrate = VAL(num\$(5))

rnumpulse = VAL(num\$(4))

framenum = VAL(num\$(6))

timeoutval = VAL(num\$(7))

timebtwx = VAL(num\$(8))

height = VAL(num\$(9))

name\$ = num\$(1)

END SUB

SUB USERDAT

LOCATE row(scr1ptr), colends(scr1ptr, 1)

CALL EDITOR(num\$(scr1ptr), colends(scr1ptr, 1), colends(scr1ptr, 2), KEYCODE,
hifore(scr1ptr), hiback(scr1ptr))

DO

SELECT CASE KEYCODE

CASE 27 'esc

CALL HILITE(nfore(scr1ptr), nback(scr1ptr), scr1ptr)

EXIT DO

CASE 13 'cr

' any thing else, just move down 1 item

```

CALL HILITE(nfore(scr1ptr), nback(scr1ptr), scr1ptr)
scr1ptr = scr1ptr + 1
IF scr1ptr > numlabel THEN scr1ptr = 1
CALL HILITE(hifore(scr1ptr), hiback(scr1ptr), scr1ptr)

LOCATE , colends(scr1ptr, 1)
CALL EDITOR(num$(scr1ptr), colends(scr1ptr, 1),
colends(scr1ptr, 2), KEYCODE, hifore(scr1ptr), hiback(scr1ptr))

CASE -80 'dn
CALL HILITE(nfore(scr1ptr), nback(scr1ptr), scr1ptr)
scr1ptr = scr1ptr + 1
IF scr1ptr > numlabel THEN scr1ptr = 1
CALL HILITE(hifore(scr1ptr), hiback(scr1ptr), scr1ptr)
LOCATE , colends(scr1ptr, 1)
CALL EDITOR(num$(scr1ptr), colends(scr1ptr, 1),
colends(scr1ptr, 2), KEYCODE, hifore(scr1ptr), hiback(scr1ptr))
CASE -72 'up
CALL HILITE(nfore(scr1ptr), nback(scr1ptr), scr1ptr)
scr1ptr = scr1ptr - 1
IF scr1ptr < 1 THEN scr1ptr = numlabel
CALL HILITE(hifore(scr1ptr), hiback(scr1ptr), scr1ptr)
LOCATE , colends(scr1ptr, 1)
CALL EDITOR(num$(scr1ptr), colends(scr1ptr, 1),
colends(scr1ptr, 2), KEYCODE, hifore(scr1ptr), hiback(scr1ptr))
CASE -77 'L
LOCATE , colends(scr1ptr, 1)
CALL EDITOR(num$(scr1ptr), colends(scr1ptr, 1),
colends(scr1ptr, 2), KEYCODE, hifore(scr1ptr), hiback(scr1ptr))
CASE -75 'R
LOCATE , colends(scr1ptr, 1)
CALL EDITOR(num$(scr1ptr), colends(scr1ptr, 1),
colends(scr1ptr, 2), KEYCODE, hifore(scr1ptr), hiback(scr1ptr))
CASE -56 'ALT
LOCATE , colends(scr1ptr, 1)
CALL EDITOR(num$(scr1ptr), colends(scr1ptr, 1),
colends(scr1ptr, 2), KEYCODE, hifore(scr1ptr), hiback(scr1ptr))
CASE ELSE
LOCATE , colends(scr1ptr, 1)
CALL EDITOR(num$(scr1ptr), colends(scr1ptr, 1),
colends(scr1ptr, 2), KEYCODE, hifore(scr1ptr), hiback(scr1ptr))
END SELECT
LOOP

```



```

FOR i = 2 TO framenum + 9
    COLOR nfore(i), nback(i)
    LOCATE row(i), colends(i, 1)
    PRINT VAL(num$(i));

NEXT

END SUB

SUB VALIDATE (request$)
count = 0
b$ = ""
RETRY:      PRINT #1, request$
            CALL DELAY
            IF INSTR(b$, "0 -->") THEN
            ELSE
                count = count + 1
                b$ = ""
                BEEP'PRINT COUNT
                IF count > 2 THEN
                    CALL CLMESS
                    PRINT "Dam,... error in validate"
                    STOP
                END IF
                GOTO RETRY
            END IF
END SUB

```

Appendix 2. Determination of the vortex ring Reynolds number

To determine the vortex ring's Reynolds number a value for the circulation Γ , is required. This is impossible to obtain directly but it can be estimated if the vortex ring velocity is known. For the present experiments the velocity was obtained using multiple exposure photographs, the exposures being taken at 15 ms intervals. An example of these photographs is shown in Figure A2.1. With reference to Figure A2.2 an estimate of the circulation was obtained using Kelvin's inviscid solution for the velocity of a vortex core with finite radius δ and vortex ring radius R , Lamb (1935).

$$U_{ring} = \frac{\Gamma}{4\pi R} \left[\log\left(\frac{8R}{\delta}\right) - \frac{1}{4} + O\left(\frac{\delta}{R}\right) \right] \quad A2.1$$

The difficulty in applying this result lies in obtaining an appropriate core radius. A lower bound of .01 was obtained for $\frac{\delta}{R}$ using the result from Batchelor (1967). This is the minimum value of $\frac{\delta}{R}$ for which the trapped streamlines of the vortex ring close on the axis of symmetry (which is the case for the vortex rings observed in these experiments). The translational velocity, $U_{ring} = 18$ cm/s, was calculated at $t = 30$ ms. It was thought that by this time the flow induced by the free surface motion would be of negligible consequence and the motion of the vortex ring was an accurate reflection of its velocity. An estimate of $\frac{\delta}{R}$ was also obtained by setting the core radius equal to the diffusive length scale $\delta = \sqrt{4\nu t}$, using $t = 30$ ms, and setting $R = .13$ cm. The radius was chosen to be the distance from the centre of the dyed spirals within the vortex ring to the axis of symmetry. Choosing the time to be 30 ms is equivalent to assuming that at time zero the vortex core was a single concentrated line vortex. Using these values gave a circulation of 4.5 cm²/s for the lower bound and 9.3 cm²/s for the upper. These values correspond to a Re of 450 and 930 respectively. Both are well within the known range of laminar vortex rings (Shariff and Leonard 1992).

If the velocity of the vortex ring is plotted vs. time it can be seen that its velocity slows with time (Figure A2.3). Saffman (1970) shows that the action of diffusion distributing vorticity away from an initially concentrated vortex ring core will slow the translation of the vortex ring as $-\log(\nu t)$.

He calculates the velocity of a viscous vortex ring as:

$$\frac{dX}{dt} = \frac{\Gamma}{4\pi R} \left[\log\left(\frac{8R}{\sqrt{4\nu t}}\right) - .558 + O\left(\frac{\delta}{R} \log\left(\frac{\delta}{R}\right)\right) \right] \quad A2.2$$

Here X is the vorticity centroid as defined as:

$$X = \frac{\int \omega_{\phi} x r^2 dx dr}{\int \omega_{\phi} r^2 dx dr} \quad A2.3$$

and ϕ is the azimuthal angle.

It is assumed in Saffman's calculation that the vorticity is initially in a concentrated core which will spread (locally) in a two dimensional manner at early times. It is apparent when equation A2.1 is compared to equation A2.2 that the core radius δ has been replaced by the diffusive length scale $\delta = \sqrt{4\nu t}$ in the leading logarithmic term. This result is valid for $\nu t \ll R^2$. This constraint ensures vorticity does not have sufficient time to diffuse to the axis of symmetry where cancellation can occur. This time corresponds to 400 ms if the vortex ring radius is taken to be .13 cm.

There is no method to quantifiably identify the location of the vorticity centroid from photographs. The leading edge of the vortex ring was used as the point of reference. The slope calculated from the velocity of the vortex ring corresponds to a circulation of 15 cm²/s for $R = .13$ cm which is greater than that predicted by Kelvin's solution. This discrepancy is likely due to errors in estimating the vortex core radius and the vortex ring radius.

It should be remembered that these calculations were used as an order of magnitude estimate only. It is hoped that more accurate techniques may be employed in the future to measure the circulation directly from the flow field.

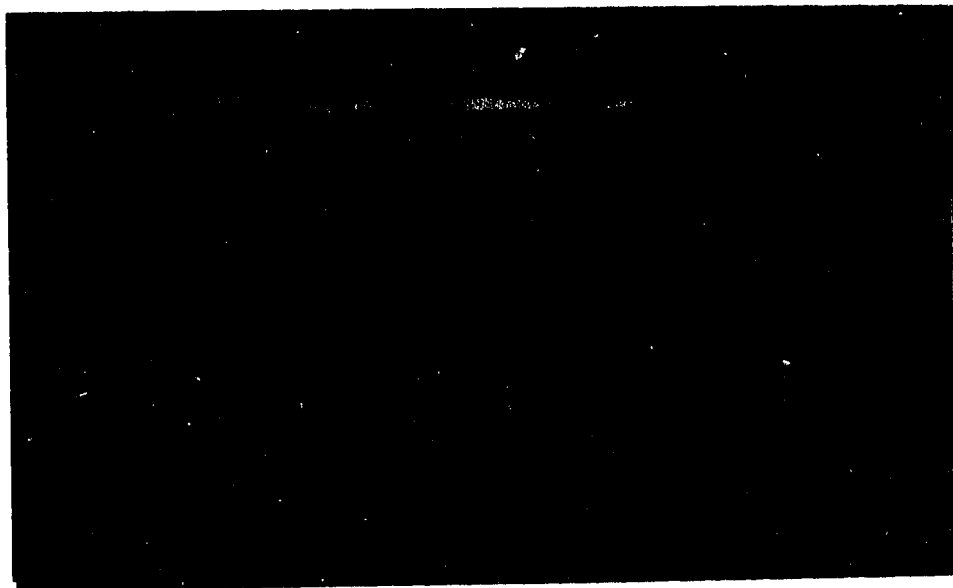


Figure A2.1. *Multiple exposure photograph of the vortex ring. Exposures are at 15 ms intervals. The orange line is caused by the laser used for timing.*

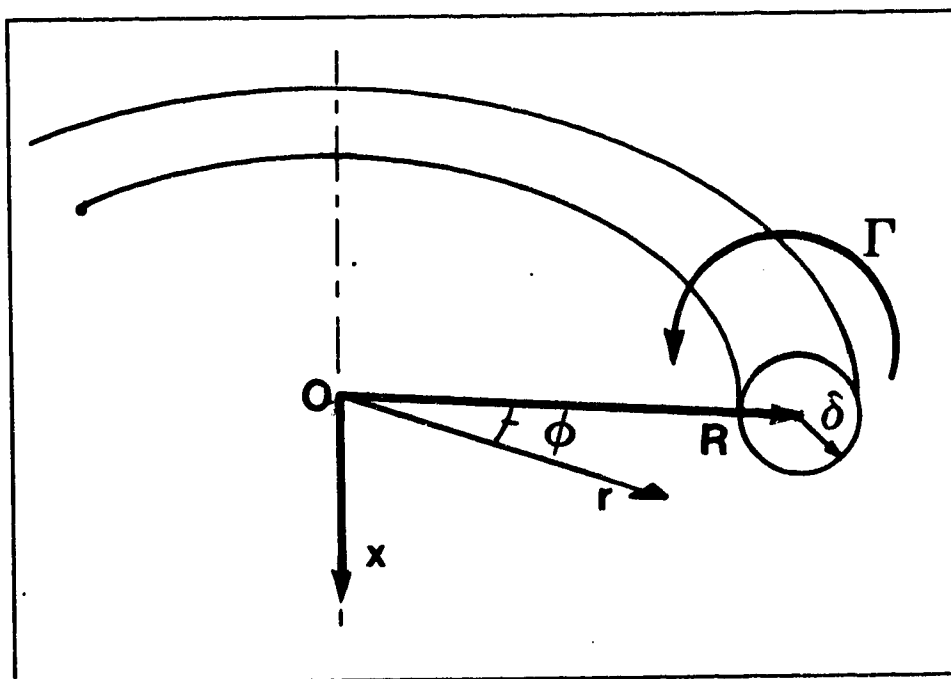


Figure A2.2. *Vortex ring geometry.*

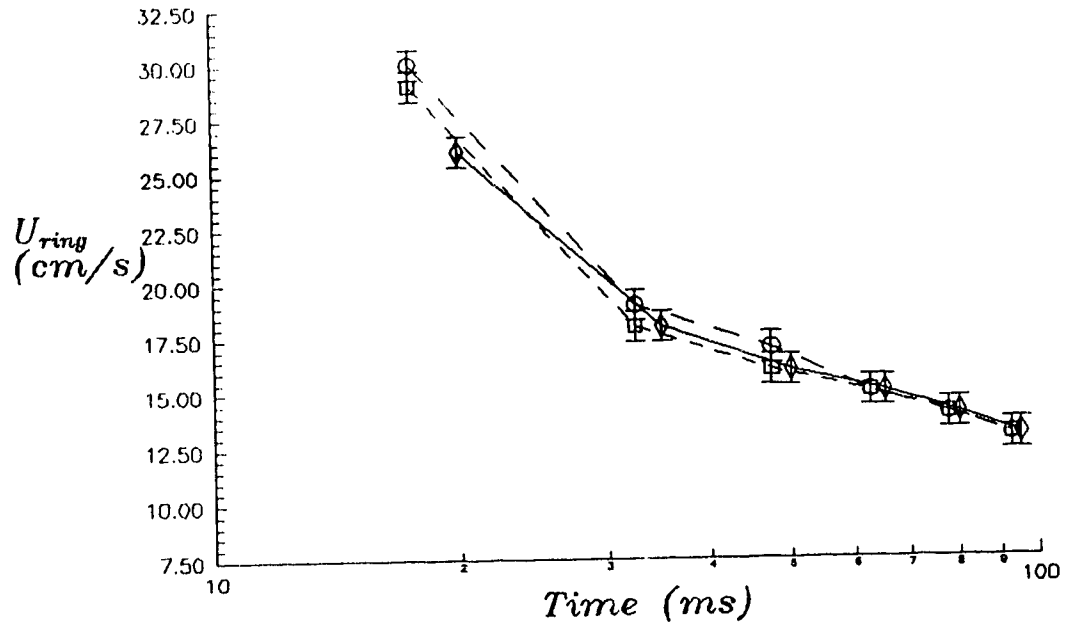


Figure A2.3. The velocity of the vortex ring vs. time for three experiments. The heavy solid line corresponds to the motion of a similar sized ring with a circulation of $15 \text{ cm}^2/\text{s}$ as calculated using equation A2.2.

Appendix 3. Vortex dynamics and vorticity generation at a free surface

A3.1 Vortex dynamics overview

The analysis of a fluid's motion can often be made simpler by tracking the vorticity distribution within it. The equation which characterizes the vorticity within the flow is derived from the Navier-Stokes equation in the following manner. It is first noted that the vorticity is defined as the curl of the velocity \mathbf{u} :

$$\boldsymbol{\omega} = \nabla \wedge \mathbf{u}, \quad (\text{A3.1})$$

and the Navier-Stokes equations (in the absence of body forces) are in the form as shown below (P =pressure).

$$\frac{\partial \mathbf{u}}{\partial t} + \mathbf{u} \cdot \nabla \mathbf{u} = -\frac{1}{\rho} \nabla P + \nu \nabla^2 \mathbf{u}. \quad (\text{A3.2})$$

To obtain the vorticity equation the curl of both sides of the Navier-Stokes equation are taken:

$$\nabla \wedge \left\{ \frac{\partial \mathbf{u}}{\partial t} + \mathbf{u} \cdot \nabla \mathbf{u} \right\} = \nabla \wedge \left\{ -\frac{1}{\rho} \nabla P + \nu \nabla^2 \mathbf{u} \right\}. \quad (\text{A3.3})$$

The left hand side can then be written as:

$$\frac{\partial \boldsymbol{\omega}}{\partial t} + \nabla \wedge \left\{ \frac{1}{2} \nabla (\mathbf{u} \cdot \mathbf{u}) - \mathbf{u} \wedge (\nabla \wedge \mathbf{u}) \right\}. \quad (\text{A3.4})$$

Noting that the second term is necessarily zero and expanding the third term yields:

$$\frac{\partial \boldsymbol{\omega}}{\partial t} + (\mathbf{u} \cdot \nabla) \boldsymbol{\omega} - (\boldsymbol{\omega} \cdot \nabla) \mathbf{u} - \mathbf{u} (\nabla \cdot \boldsymbol{\omega}) + \boldsymbol{\omega} (\nabla \cdot \mathbf{u}). \quad (\text{A3.5})$$

The divergence of the vorticity (the curl of the velocity) is also necessarily zero requiring the fourth term to vanish. For an incompressible fluid the divergence of \mathbf{u} is also zero in which case the fifth term vanishes.

If the curl of the term containing the pressure is now considered:

$$\nabla \wedge \left\{ -\frac{1}{\rho} \nabla P \right\} = - \left\{ \nabla \left(\frac{1}{\rho} \right) \right\} \wedge \nabla P - \frac{1}{\rho} \{ \nabla \wedge \nabla P \}, \quad (\text{A3.6})$$

it can be seen that the last term vanishes and the first term on the right hand side can be rewritten as:

$$\frac{\nabla \rho \wedge \nabla P}{\rho^2}. \quad (\text{A3.7})$$

This is commonly referred to as the baroclinic term and is zero if the density is constant throughout the fluid. In the case of constant density, which is the case for many incompressible flows, the vorticity equation has the advantage of eliminating the need for knowledge of the pressure distribution within the flow.

Taking the curl of the last term on the right hand side of the Navier-Stokes equation yields a similar term for the vorticity:

$$\nabla \wedge \{ \nu \nabla \cdot \nabla \mathbf{u} \} = \nu \nabla^2 \boldsymbol{\omega}. \quad (\text{A3.8})$$

This shows that vorticity is transported through the action of viscosity in a manner similar to the transport of velocity.

The vorticity equation for a homogeneous incompressible fluid can now be written as:

$$\frac{\partial \boldsymbol{\omega}}{\partial t} + (\mathbf{u} \cdot \nabla) \boldsymbol{\omega} = (\boldsymbol{\omega} \cdot \nabla) \mathbf{u} + \nu \nabla^2 \boldsymbol{\omega}. \quad (\text{A3.9})$$

There is an obvious similarity to the Navier-Stokes equations with the exception of the absence of the pressure and the appearance of the first term on the right. This is the stretching and tilting term sometimes referred to as the "tornado term". If viscosity is neglected the vorticity equation can be written as:

$$\frac{D \boldsymbol{\omega}}{Dt} = (\boldsymbol{\omega} \cdot \nabla) \mathbf{u}. \quad (\text{A3.10})$$

Considering a material line PQ initially aligned with a segment of a vortex line along which there is an incremental change in the velocity vector between the endpoints, $\delta \mathbf{u}$, the equation can be written as follows:

$$\frac{D\boldsymbol{\omega}}{Dt} = |\boldsymbol{\omega}| \lim_{PQ \rightarrow 0} \frac{\delta \mathbf{u}}{PQ}. \quad (\text{A3.11})$$

It can be seen that an incremental change of the velocity component along the material line's axis will tend to intensify the vorticity component along the line element PQ (stretching). An incremental change of the velocity component normal to the axis will cause an alteration of the vorticity due to the rigid rotation of the line element PQ (tilting). It is this term which makes the study of three-dimensional vortex structures distinctive.

Using the well known result from Kelvin for an inviscid fluid of constant density:

$$\frac{D\Gamma}{Dt} = 0 \quad (\text{A3.12})$$

where the circulation Γ is defined as:

$$\Gamma = \oint_c \mathbf{u} \cdot d\mathbf{l} \quad (\text{A3.13})$$

it can be shown that a vortex-tube's strength will remain constant in the absence of viscosity. It can also be shown by using this result that the vortex-tube will convect with the fluid in the manner of a vortex-line. It is also apparent that a stretching of the tube will cause an intensification of the vorticity within it. This result is derived by Batchelor (1967):

$$\frac{\omega(t)}{|\omega(t_0)|} = \frac{\delta l(t)}{|\delta l(t_0)|} \quad (\text{A3.14})$$

here l is a short element of length along a vortex-line. For two-dimensional flows the stretching term is zero since the velocity gradients are necessarily normal to the vorticity. The equation can then be reduced to the scalar equation:

$$\frac{D\omega}{Dt} = \nu \nabla^2 \omega \quad (\text{A3.15})$$

It is useful when considering vorticity distributions which are locally two-dimensional. This equation is analogous to the transport of dye throughout the fluid of concentration C and diffusivity K :

$$\frac{DC}{Dt} = K \nabla^2 C. \quad (\text{A3.16})$$

If the fluid's kinematic viscosity is divided by the diffusivity of the dye the Schmidt number, $Sc = \frac{\nu}{K}$, is obtained, which is approximately 50 for water. It can be seen that the vorticity will be transported by diffusion through the fluid at a much higher rate than the dye. Thus if an individual line vortex is chosen which is initially dyed the vorticity within it will diffuse away from the line quicker than the dye.

The Biot-Savart law will be stated below for an incompressible flow without proof, a derivation of this relation is given in Batchelor (1967). The Biot-Savart law gives the velocity field if the vorticity field and any base potential flow present are known.

$$\mathbf{u}(\mathbf{x}) = -\frac{1}{4\pi} \int_{vol} \frac{(\mathbf{x}-\mathbf{x}') \wedge \boldsymbol{\omega}(\mathbf{x}')}{|\mathbf{x}-\mathbf{x}'|^3} dV(\mathbf{x}') \quad (\text{A3.17})$$

It should be noted here that the primes refer to the portion of the element within which the vorticity is associated while the non-primed positions are the points where the velocities are being calculated.

For a line vortex this equation can be written as

$$\mathbf{u}(\mathbf{x}) = -\frac{\Gamma}{4\pi} \int_l \frac{(\mathbf{x}-\mathbf{x}') \wedge d\mathbf{l}(\mathbf{x}')}{|\mathbf{x}-\mathbf{x}'|^3} \quad (\text{A3.18})$$

This kinematic result can then be used to determine the flow field if the flow is modelled as a series of line vortices. It can be seen that this result would be of great utility in determining the motion of other line vortices as a consequence of Kelvin's Theorem stated earlier when applied to a line vortex. This theorem ensures that the circulation will remain constant along the line vortex reducing the problem to one of geometry. If the line vortex is curved the formula can not give the velocity of all the points on the line vortex itself. It can be seen the result will become infinite as $x-x'$ becomes small. Thus the calculation must be terminated as x approaches x' . The value at which this calculation is terminated is termed the cutoff and can introduce an error into the calculation.

Two geometries will now be briefly discussed, the vortex ring and the hairpin or Lambda vortex. In both cases a suitable cutoff will be assumed. For the case of the vortex ring it can be seen from the Biot-Savart law that each point on the vortex ring will induce a velocity in the rest of the ring so as to propel the circular line vortex along the axis of symmetry. It can also be deduced that two rings of equal dimension and circulation approaching one another will radially expand, increasing their circumference as they come closer to one another.

Two rectilinear line vortices of opposite sign equally spaced along their length will propel each other in a direction perpendicular to their length (for line vortices of infinite extent). If such a pair is considered which is closed on one end by what may be viewed as one half of a vortex ring, the curvature of the line will now allow the self propagation of the line vortex, in this region of curvature, to be enhanced, propelling the tip of the vortex faster than the length creating an arching of the line vortices. This is responsible for the characteristic shape observed in the petals of the three-dimensional vortex structure considered in these experiments.

In two-dimensions, several flows have been examined analytically and the reader is referred to Lamb (1945) and Batchelor (1967) for exhaustive solutions to many of these flows.

A3.2 Vorticity generation at a free surface

If a flow is to be examined by tracking the evolution of its vorticity, the initial distribution of the vorticity must be known for a complete understanding of the problem. This often requires knowledge of the vorticity generation mechanism. In the problem studied here the generation mechanism is not well understood although it is thought to be due to the presence of the free surface. The generation of vorticity at a free surface is not a well understood subject in general and is presently the subject of a great deal of research.

If the falling drop is considered just prior to the moment of impact, the drop and the quiescent pool will possess different velocity potentials. It follows that as the drop and pool coalesce a sheet of vorticity must exist between the discontinuous velocities. This does not explain the dynamical means by which the torques are generated to create the vorticity. This situation is analogous to the popular but misguided belief that the vorticity in a shear layer is generated by "the shear in the fluid caused by the discontinuous velocities". This is false; in an incompressible fluid the vorticity must be generated at a boundary. For shear layer experiments this is typically at a splitter situated upstream. No vorticity can be generated within an incompressible fluid with constant density in the absence of boundaries. The vorticity must be present in both cases just mentioned to match the discontinuous velocities, but this does not explain its production.

In the drop impact problem the presence of the free surface introduces a discontinuous density at the interface. As a result the vorticity which must be present may be generated by baroclinic torques set up by tangential pressure gradients. Due to the small drop height of the impacting drop experiments studied here it is likely that the vorticity generation mechanism derives much of its energy from the surface tension of the drop. This is demonstrated by the formation of a vortex ring from a pendant drop slowly being lowered to touch a pool. In this situation the available surface energy for a 2.6 mm drop is 10 times that of its potential energy indicating that it is the contraction

of the free surface which applies most of the necessary impulse for vorticity production. Even for the same sized drops released from 35 mm the available surface energy is still over half of the kinetic energy at impact. While production of the necessary torques is not understood it will be shown that the presence of free surface curvature and a tangential fluid velocity requires the presence of vorticity.

Longuet-Higgins (1992) derives the following relationship for the jump in vorticity across the boundary layer which forms at the free surface in a steady two-dimensional flow:

$$\Delta \omega = 2\kappa q \quad (\text{A3.19})$$

Here κ is the curvature of the free surface, q is the magnitude of the tangential component of velocity. This equation also appears in a more general form in Longuet-Higgins (1953). This equation leads him to the following statement, "that any curved free surface in a steady flow, irrotational or not, is necessarily a source of vorticity".

The derivation proceeds as follows. With reference to Figure A3.1, the vorticity is considered with respect to a fixed set of axes (x,y) and the associated velocities (u,v) :

$$\omega = \frac{\partial v}{\partial x} - \frac{\partial u}{\partial y} \quad (\text{A3.20})$$

The tangential stress is given by:

$$\tau_{ns} = \mu \left(\frac{\partial u}{\partial y} + \frac{\partial v}{\partial x} \right) \quad (\text{A3.21})$$

Here n and s are the normal and tangential directions along the free surface. There is also the no-slip condition at the free surface. This requires the tangential stress applied to be continuous across the interface. This implies that there is a jump in the velocity derivative across the interface. At the air-water interface the low viscosity of air allows this condition to be approximated as a zero tangential stress.

Setting the shear stress to zero:

$$\frac{\partial u}{\partial y} = -\frac{\partial v}{\partial x} \quad (\text{A3.22})$$

Substituting into equation A3.2 yields:

$$\omega = 2 \frac{\partial v}{\partial x} \quad (\text{A3.23})$$

The axes (s,n) are now taken to be tangential and normal to a streamline on the boundary of the irrotational bulk flow at a point P where θ is the angle of rotation from (x,y). Then:

$$v = q \sin\theta \quad (\text{A3.24})$$

and

$$\frac{\partial}{\partial x} = \cos\theta \frac{\partial}{\partial s} + \sin\theta \frac{\partial}{\partial n}. \quad (\text{A3.25})$$

Differentiating with respect to the new axis yields:

$$\frac{\partial v}{\partial x} = \sin\theta \cos\theta \frac{\partial q}{\partial s} + q \cos^2\theta \frac{\partial \theta}{\partial s} + q \cos\theta \sin\theta \frac{\partial \theta}{\partial n} + \sin^2\theta \frac{\partial q}{\partial n} \quad (\text{A3.26})$$

Setting $\theta = 0$ and noting that the surface curvature is given by $\kappa = \frac{\partial \theta}{\partial s}$ yields:

$$\frac{\partial v}{\partial x} = \kappa q. \quad (\text{A3.25})$$

A3.1 is recovered when this result is substituted into A3.5. This gives the amount of vorticity which must be present across the boundary layer at the free surface.

An elegant physical interpretation is provided for this situation. A radius is drawn from the centre of the surface curvature to a fluid element along the surface with tangential velocity q (Figure A3.2). The required absence of tangential stress ensures the element will not deform and thus the element must be in rigid body rotation with

angular velocity Ω . The vorticity, ω , is then 2Ω . Expressing Ω as $\frac{1}{r}$ and noting that $\kappa = \frac{1}{r}$ yields equation A3.1 again.

This result is derived based on the assumption of two-dimensional steady flow. A more general three-dimensional result is given by Batchelor (1967). It is shown to be reducible to equation A3.1 in two dimensions.

Through the numerical experiments of Ohring and Lugt it was shown that a qualitative understanding of the vorticity generation at a free surface in an unsteady flow can be achieved by examining the location of the surface curvature. The computer simulation begins with a vortex pair rising toward a free surface (Figure A3.3). As the pair moves closer to the free surface the surface is deformed and vorticity is generated. Vorticity of the same sign as the nearby vortex is generated at regions of positive curvature (the radius of curvature lies within the fluid), while opposite signed vorticity is generated at the region of changing curvature (Figure A3.4). The tangential flow required for the presence of vorticity is a consequence of the Biot-Savart induced velocity field. The stronger pairs examined show the vorticity to separate at regions of high curvature referred to as a scar.

Separation of the boundary layer from the free surface allows vortical fluid to convect into the flow. In Ohring and Lugt's work the flow separates at the trailing edge of the scar, the vorticity evidently being generated upstream. Periodic shedding of vortices is mentioned that is similar to that observed from solid bodies. This may or may not be useful in understanding the number of base rings which form in the reversing impact crater of the drop experiment. Free surface boundary layer separation is also observed in the wake of a rising bubble cap. In this geometry the boundary layer separates at the region of highest curvature or the lip of the bubble cap. Much remains to be learned in the area of free surface boundary layer separation.

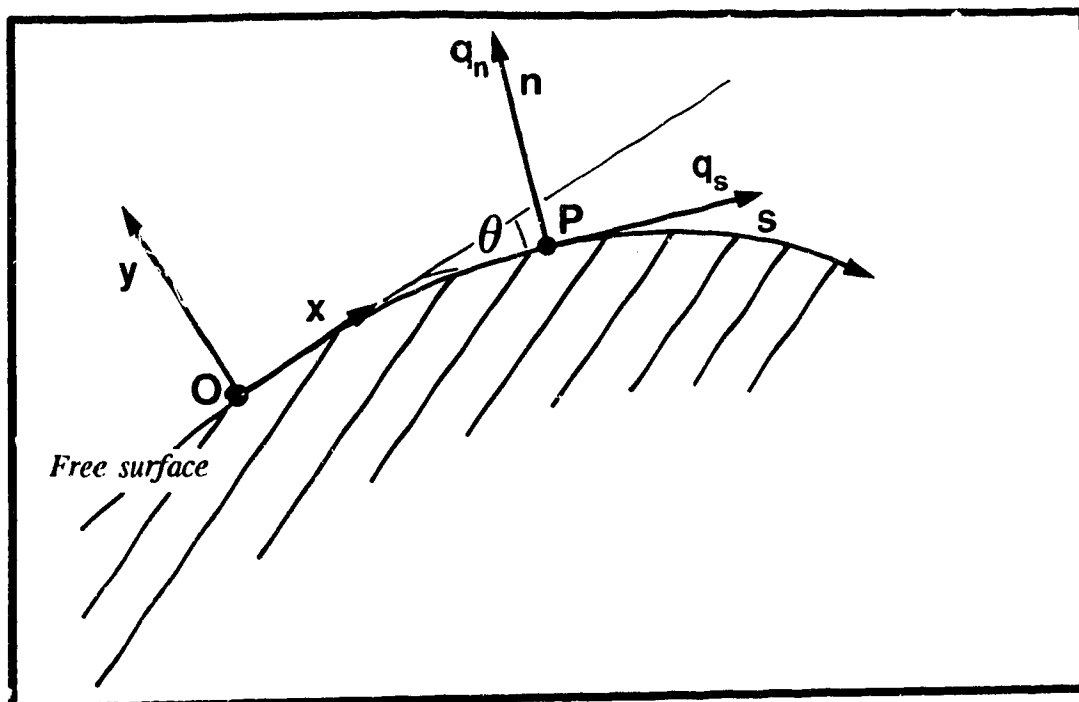


Figure A3.1 *Coordinate systems at free surface.*

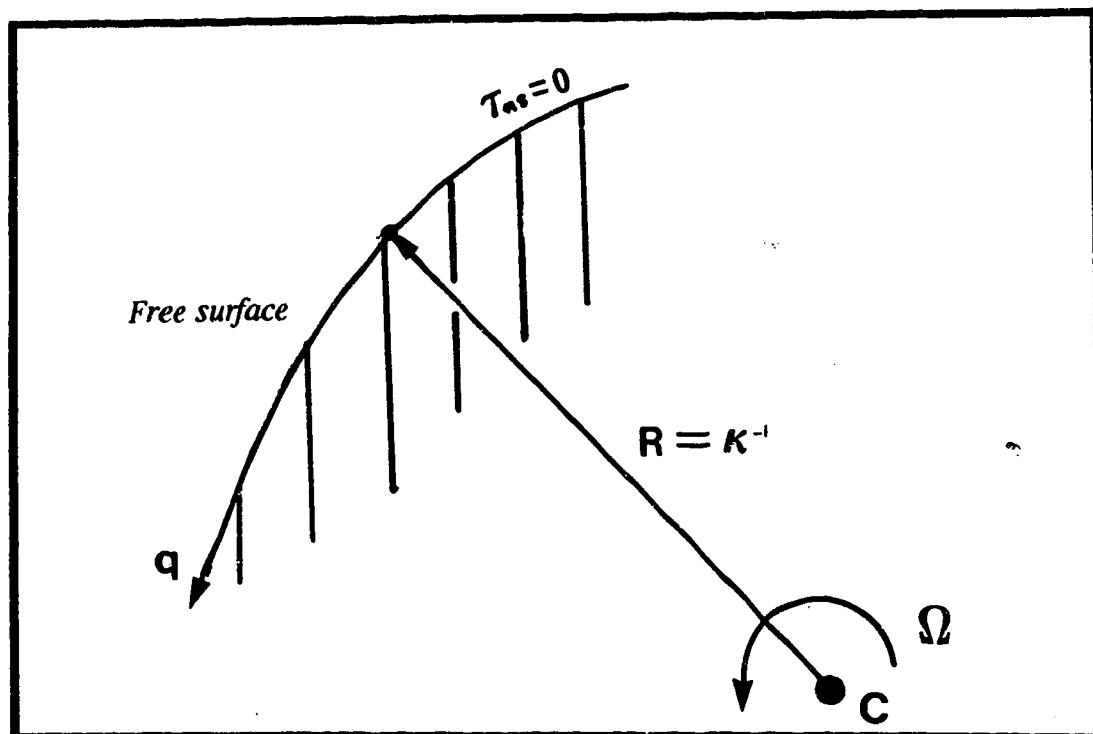


Figure A3.2 *Region of curvature at a free surface where fluid must be in solid body rotation.*

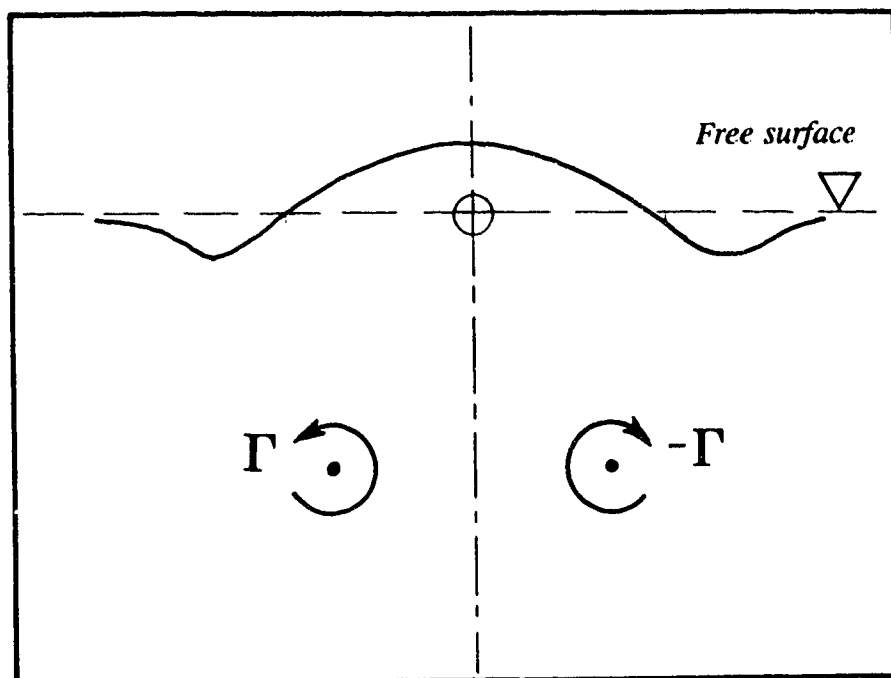


Figure A3.3 Sketch of flow geometry in the computations of Ohring and Lugt (1990).

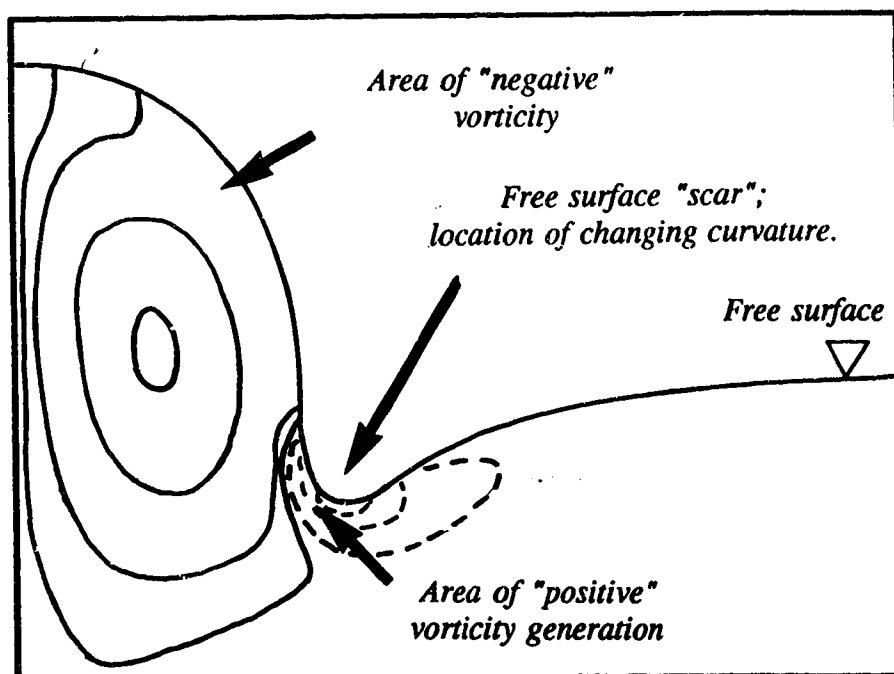


Figure A3.4 Sketch of equivorticity lines as calculated by Ohring and Lugt. Solid lines indicate negative vorticity while dashed lines indicate positive vorticity.